A Fracture ~~Never~~ Rarely Comes Alone: Associations of Fractures and Stylolites in Analogue Outcrops Improve Borehole Image Interpretations of Fractured Carbonate Geothermal Reservoirs

Jasper Hupkes[1], Pierre-Olivier Bruna[1], Giovanni Bertotti[1], Myrthe Doesburg[1], and Andrea Moscariello[2]

[1]Department of Geoscience and Engineering, Delft University of Technology, Delft, The Netherlands
[2]Department of Earth Sciences, University of Geneva, Geneva, Switzerland

Correspondence: Jasper Hupkes (j.hupkes@tudelft.nl)

Abstract. ~~Natural discontinuity networks control convective fluid flow in carbonate geothermal reservoirs with low matrix porosity and permeability. The network can be separated into discontinuities that formed due to local drivers (e.g. faults/folds) and the background network formed by far-field stresses, each with different scaling behaviour. Borehole data are the only source to sample the subsurface network, as the majority of the discontinuities are of sub-seismic scale. Borehole images are the most cost-effective way of sampling the network, but the limited sample area and image resolution hamper the identification of the background network in this dataset. Analogue outcrops may complement the borehole data, but only after the analogy between outcrop and subsurface reservoir is established.~~ In this study, we present a method that uses associations of discontinuity sets to establish ~~a robust link~~ the analogy between the outcrop and the subsurface. A discontinuity association comprises up to ~~4 discontinuity sets~~ four discontinuity sets (fractures and stylolites) that can form coeval in a single stress field, a well-known concept that is rarely applied for subsurface characterization of discontinuities. We use ~~the orientations and type of discontinuity associations as paleostress indicators in order to map out principal stress trajectories of regional discontinuity-forming events that created the background discontinuity network. We demonstrate this methodology~~ this concept to improve the interpretation of borehole image logs of naturally fractured geothermal reservoirs in the Geneva Basin, Switzerland~~, where~~. Here, the naturally fractured Lower Cretaceous pre-foredeep ~~carbonates~~ carbonate rocks are targeted for geothermal exploitation~~. Outcrops in the~~, and exposures of this formation are found in three mountain ranges that surround the basin~~, consistently reveal~~. In these outcrops, the orientations of the discontinuity associations are used as paleostress indicators in order to map out principal stress trajectories of regional discontinuity-forming events that created the background discontinuity network. We document two multiscale discontinuity-forming events that formed prior to Alpine fold-and-thrusting and thus constitute the regional scale background network. ~~Therefore, based~~ Based on the analogy principle, we predict that the target reservoir is also affected by these events. ~~We use this prediction to isolate~~ This prediction is subsequently used to isolate the background-related discontinuities on image logs from two boreholes that penetrate the target reservoir in the Geneva Basin. This analysis reveals that ∼45% of the observed discontinuities can be understood in the framework of the regional-scale background. In this way, we demonstrate that ~~DAs in outcrops are~~ defining discontinuity associations in outcrops is a powerful tool to predict the geometry of natural discontinuity networks in the subsurface and subsequently can be used to develop geothermal exploitation strategies in naturally fractured reservoirs.

1 Introduction

~~Natural discontinuity networks (NDNs) control convective heat flow in fractured~~ Carbonate geothermal reservoirs with a low matrix porosity and permeability ~~(Berre et al., 2019; Medici et al., 2023). Discontinuities~~ may still have a convective heat flow due to the presence of natural discontinuity networks (NDNs) (Berre et al., 2019; Medici et al., 2023). Natural discontinuities (fractures and stylolites) can create a heterogeneous reservoir permeability by either forming preferred flow pathways or ~~flow barriers (Bruna et al., 2019; La Bruna et al., 2021).~~ barriers (e.g. Caine et al., 1996; Solano et al., 2011; Grare et al., 2018; Fadel et al., 202 . Also, natural discontinuities impact the rock strength, which is essential to consider in the case of hydraulic stimulation of a reservoir (Cao and Sharma, 2022; Rysak et al., 2022). Predicting the geometry of NDNs in the subsurface is therefore crucial to avoid production risks such as early thermal breakthrough (Fadel et al., 2023) and/or induced seismicity (Zang et al., 2014; Atkinson et al., 2020).

A ~~common approach to analyze NDNs is by breaking the network down into discontinuity sets (Peacock et al., 2018). The definition of a set is based on the orientation of the discontinuities and, if possible to determine, the discontinuity type. These sets can be separated based on their geomechanical driver. Their formation is either related to local drivers such as folds and faults (Price, 1966; Torabi and Berg, 2011) or to regional, far-field stresses (Lamarche et al., 2012; Bertotti et al., 2017; Lavenu and Lamar . Discontinuities formed by the latter constitute the background network. The spatial distribution of the intensity of the discontinuities is partially controlled by the driver. For local drivers, discontinuities concentrate where strain accumulates (e.g. in the damage zone or fold hinge), whereas the background network is more homogeneously distributed.~~

~~The majority of the discontinuities~~ large portion of the discontinuities are of sub-seismic scale. ~~Seismic data can aid the prediction of the sub-seismic discontinuities in the subsurface related to local drivers, if faults and/or folds are above the seismic resolution (Maerten et al., 2006). Predicting the background network based on seismic data however remains challenging, as there are no seismic-scale structures related to this part of the network.~~ The only way to directly observe ~~sub-seismic scale discontinuities of the background network~~ these discontinuities in the subsurface is through borehole data. These data classically consist of cores and borehole images. Borehole images (BHI) are a cost-effective alternative to core data, enabling classification of discontinuities based on their structural attitude (dip and strike) and their geophysical responses ~~(filled – resistive or open - transmissive) (Williams and Johnson, 2004)~~(filled — resistive or open — transmissive Williams and Johnson, 2004) . However, ~~the~~ there are several limitations to the usefulness of BHI-interpretations: for example, the resolution of BHIs ~~may hinder the~~ inhibit identification of discontinuity type, ~~which is crucial to interpret the geomechanical driver of the discontinuity~~and separating drilling-induced from natural fractures is not straight-forward (e.g. Lorenz and Cooper, 2017; Chatterjee and M . On top of ~~this, the sampling area (diameter of the borehole) is too small to observe the relationship between individual discontinuities and local structures such as faults and folds. This prevents the separation in the borehole of background-related discontinuities from those that formed due to local stresses~~that, it is challenging to place individual features observed on BHI into a broader context such as the reservoir, as different fracture histories may have resulted in the same fracture geometry observed at present-day (i.e., equifinality, see Laubach et al., 2019).

In contrast, outcrop studies allow to characterize the Because of the limitations of BHI data, outcrops are used as an additional source to characterize key attributes of discontinuities that are necessary to retrieve the geological driver responsible of their formation. But to use the outcrop for subsurface characterization of NDNsthe discontinuity network, such as length, spacing and connectivity in the subsurface (e.g. Agosta et al., 2010; Sanderson, 2016; Ukar et al., 2019). However, the analogy between the two domains needs to be established (Peacock et al., 2022). Besides outcrop and subsurface is far from trivial (e.g Bauer et al., 2017; Peacock et al., 2022). To establish the analogy between outcrop and subsurface, not only similar lithology and age of formation , a shared tectonic history is importantfor establishing such analogy (Petit et al., 2022) . As the background network is the result of regional, far-field stresses, it is likely that both outcrops and the subsurface preserved discontinuities related to these regionalstressesis preferential, but also the diagenetic evolution and/or the evolution of mechanical properties (Bruna et al., 2019; Petit et al., 2022; Elliott et al., 2025) and tectonic history (e.g. Engelder, 1985; English, 2012; P are important. Therefore, the orientation of the stress field that produced the background network can potentially function as the link between outcrop and subsurface. For the latter, a comparison of the stress evolution of outcrop and subsurface is needed.

In outcrop studies, attempts have been made to group discontinuities based on the tectonic driver (e.g. Beaudoin et al., 2013; Aubert et al. . Their formation is either related to local drivers such as folds and faults (Price, 1966; Torabi and Berg, 2011) or to regional, far-field stresses (e.g., Bergbauer and Pollard, 2004; Casini et al., 2011; Lamarche et al., 2012; Bertotti et al., 2017; Lavenu and Lamarche . Discontinuities formed by the latter constitute the background network (sometimes called diffuse fractures). The distinction between drivers is relevant, as the spatial distribution and the intensity of the discontinuities is partially controlled by the driver. For local drivers, discontinuities concentrate where strain accumulates (e.g. near the fault damage zone or fold hinge), whereas the background network is present throughout the reservoir, with a spatial variability likely related to bed thickness, mechanical stratigraphy and diagenetic processes at time of fracturing (Bai and Pollard, 2000; Laubach et al., 2009; Chemenda, 2022; Procter and Sanc . Understanding the genetic origin of discontinuities is therefore essential for extrapolation of discontinuity geometry to reservoir scale.

Stress fields in which discontinuities formed may be deployed to unravel the genetic origin of the discontinuity. There are various methods that use discontinuities for paleostress inversion(Angelier, 1990; Maerten et al., 2016; Pascal, 2021), either based on slip vectors (e.g. Angelier, 1990; Maerten et al., 2016; Pascal, 2021), or shape of stylolites (e.g. Beaudoin et al., 2016; Toussaint et al., 2 . Associations of discontinuities that formed coeval in a single stress field are more robust indicators than single discontinuity sets 2 (Hancock, 1985)(see figure 2, Hancock, 1985). The concept that multiple discontinuity sets can form in a single stress field is largely sensed by structural geologist (e.g. Groshong, 1975), but surprisingly little used to establish the analogy between outcrop and the subsurface. This notion gives additional value to the surface study, as it may provide provides a geological context for the interpretation of BHI-data from discontinuities in the target reservoir. The derived paleo principal stresses that caused the formation

In this study, we use outcrops to predict the geometry of the background network as observed in the field can be used to predict the orientation of discontinuities in the subsurface . Based on the predicted orientations, background-related discontinuities in the borehole can be separated from those that formed by other, local mechanisms. The regional nature of the background network allows the extrapolation of these discontinuities away from the borehole and even beyond the limits of the targeted

reservoir. In this way, investigating analogue outcrops can minimize the risks of further exploitation of the targeted geothermal reservoir.

In this study, the concept of using associations of background discontinuities in the subsurface of the Geneva Basin, Switzerland. We propose a methodology that utilizes associations of fractures and stylolites as the link between outcrop and target reservoirsubsurface reservoir. This concept is applied to the pre-foredeep Lower Cretaceous limestone in the Geneva Basinlimestones. Recently, the Canton of Geneva supported different geothermal projects to exploit the subsurface of the Geneva Basin for cooling and heating applications (Geothermies https://www.geothermies.ch/, Heatstore https://www.heatstore.eu/). In the scope of these projects, two wells (GEo-01 and GEo-02) have recently been drilled in the basin for geothermal exploration of the Mesozoic carbonates carbonate rocks in the basin (Guglielmetti et al., 2021). Borehole data (including borehole images) of the two wells have shown that the Lower Cretaceous formations in particular are a potential geothermal reservoirdue to a high, natural fracture-related permeability , in spite of having a low primary porosity (<10%) and permeability (<0.1 mD) (Rusillon, 2017; Brentini, 2018; Moscariello, 2019; Clerc and Moscariello, 2020; Guglielmetti and Moscariello, 2021). Outcrops of the Lower Cretaceous are found on both the northwestern, southwestern and southeastern

Based on the documentation of discontinuity associations in the outcrops, two events are defined that formed prior to tilting of the strata, and are consistently observed on different sides of the basin. The reconstructed stress trajectories of the two events are subsequently used to predict the geometry of the background network in the target reservoir. With this prediction, discontinuities related to the background network are identified on the borehole images of the two wells that penetrate the target reservoir. ~45% of the discontinuities visible on the BHI fit within the predicted background network. This shows that grouping fractures and stylolites into associations provides valuable information for the characterization of the subsurface discontinuity network. The regional character of the background network can be used in future geothermal explorations in the Geneva Basin. Furthermore, the proposed methodology may serve as a guideline for any exploration project of a fractured geothermal reservoir.

2 Geological Background

The Geneva Basin is located in the western part of the Swiss Molasse Basin/North Alpine Foreland Basin (figure 1, Jura Mountains , Vuache Range and Parmelan/). It is bounded by the Jura Mountains in the northwest, the Salève Range respectively). In these outcrops, we isolate the discontinuities of the background network that formed due to far-field stresses, focusing only on the associations of discontinuities that formed prior to Alpine fold-and-thrusting that shaped the present-day mountain ranges. Subsequently, we reconstruct regional paleostress trajectories to establish the analogy between outcrop and target reservoir, and thus enable the prediction of in the southeast and the Vuache range in the southwest. In the geometry of subsurface of the basin, the background network in the subsurface. We use the results of the outcrop study in our discontinuity interpretation of the BHI of the two wells in the target reservoir to quantify the portion of the background network compared to the total network. The results provide valuable information for future geothermal explorations in the area. Mesozoic strata are dipping 10° to 20° to the southeast. The depth of the top of the Lower Cretaceous increases from surface exposures in the

northwest (Jura Mountains) to ~1400 m in the southeast at the foot of the Salève Range (Jenny et al., 1995; Guglielmetti et al., 2020) .

At present-day, exposures of the Lower Cretaceous are found in the mountain ranges surrounding the Geneva Basin and the Bornes Massif, part of the Sub-Alpine Chain (figure 1). In the Parmelan, part of the Bornes Massif, the Lower Cretaceous carbonates are exposed in the flat-lying plateau and steeply-dipping limbs of a box-fold (Berio et al., 2021). The largest exposure is on the plateau with a size of ~2.5x2 km where the bedding is sub-horizontal and largely barren of vegetation. The box-fold is underlain by a NW-vergent thrust (Bellahsen et al., 2014) that structurally separates it from the Salève Range in the northwest. The Salève Range is also positioned above a NW-vergent thrust that marks the southeastern boundary of the Geneva Basin (Charollais et al., 2023). Here, the Lower Cretaceous is exposed in small outcrops (~10 meters) on the SE-dipping limb of this range. On the other side of the Geneva basin, the Jura Mountains contains several Lower Cretaceous exposures, typically in the river valleys, along road cuts and in abandoned quarries. The outcrop sizes vary between several meters to 100 meter. The mountain range is shaped by NW-verging folds and thrust formed by thin-skinned deformation (Homberg et al., 2002; Sommaruga et al., 2017). The Vuache Fault is part of a system of sinistral strike-slip faults related to the NW-vergent thrusting in the Jura (Homberg et al., 2002; Smeraglia et al., 2022). Transpression along this fault gave rise to the Vuache Range, with several exposures of the Lower Cretaceous carbonates along road cuts, with outcrop size up to ~10 meters.

The Lower Cretaceous formations consists predominantly of carbonates, with intercalations of marl layers (Rusillon, 2017; Strasser et al. . They are deposited in a branch of the Tethys Ocean (Clavel et al., 2007, 2013), and initially buried in the Late Cretaceous. The maximum depth during this first burial phase is poorly constrained, with estimates ranging from 800-1800 m in the Geneva Basin (Schegg and Leu, 1998), and up to 2000 m in the Sub-Alpine chain (Butler, 1991). Exhumation during the Paleocene led to sub-aerial exposure of the Lower Cretaceous carbonate rocks (Crampton and Allen, 1995). A second burial cycle placed the beneath Eocene to Pliocene molasse sediments in the foredeep of the Alpine Orogeny, whose thickness tapers towards the northwest. The estimated maximal burial depths of this second burial phase range between 2000 m in the Geneva Basin (Schegg and Leu, 1998) and 4000 m in the Bornes Massif (Butler, 1991; Moss, 1992; Deville and Sassi, 2006). In the Early Miocene, shortening in the Western Alps was accommodated by different folds and thrusts with a northwest vergence (Kalifi et al., 2021; Marro et al., 2023), ultimately leading to the exhumation of the Lower Cretaceous in the present-day mountain ranges in the Pliocene (Cederbom et al., 2004). Based on stress inversion of focal mechanisms in the Geneva Basin, the present-day stress field is pure strike-slip with $\sigma 1$ oriented NW-SE (Antunes et al., 2020).

3 Methodology

3.1 Grouping Discontinuities into Associations

~~Our approach~~ The approach used in this study is based on outcrop observations of discontinuities, namely ~~mode I and mode II fractures, vein~~ opening-mode fractures, shear fractures, fracture arrays and stylolites, that are genetically associated with a certain stress field (figure 2). Discontinuity sets are defined on the basis of both orientation and discontinuity type

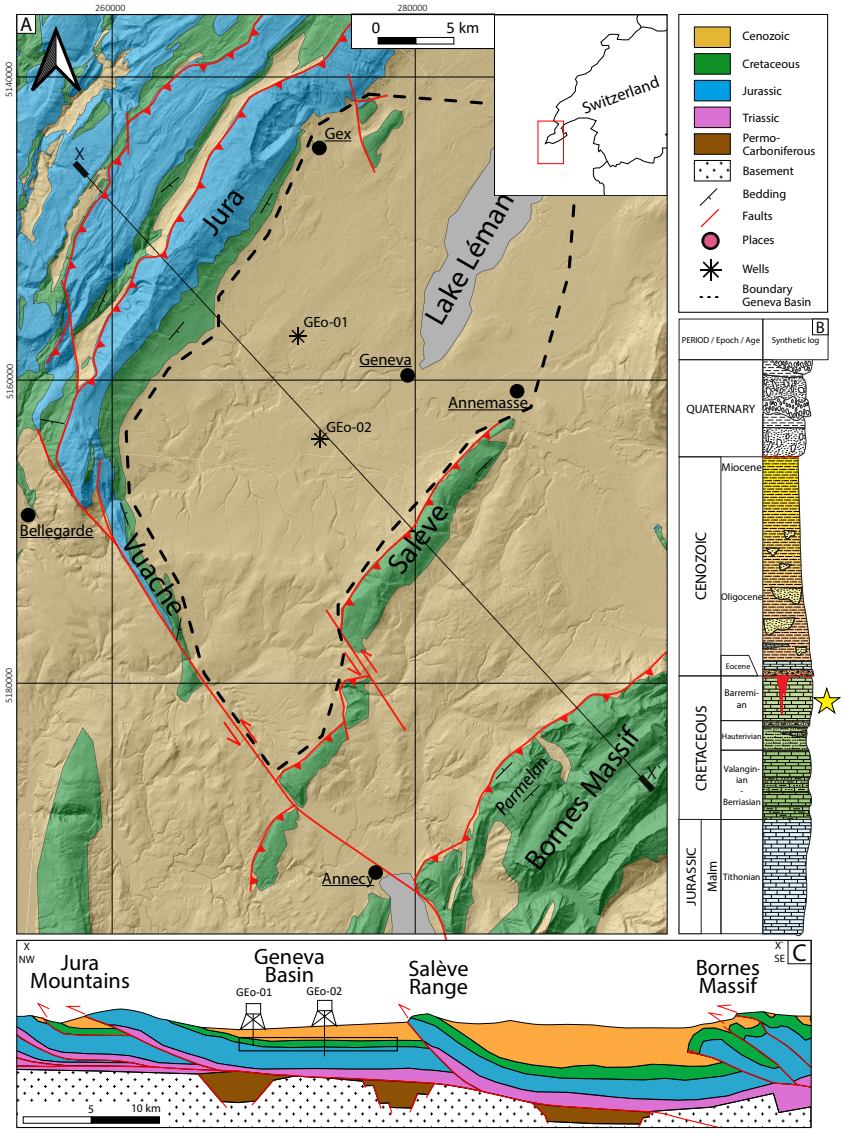

Figure 1. A) Simplified geological map modified after the 1:200.000 geological map of the Swiss Federal Office of Topography. The Geneva Basin (dashed black line) is located at the most western termination of the North Alpine Foreland Basin. Analogue outcrops of the Lower Cretaceous target reservoir are found in the Jura, Vuache, Salève and Bornes Massif (Parmelan) mountain ranges. Coordinates in UTM 32N reference frame. B) Synthetic log of the sedimentary succesion in the Geneva Basin, from the Upper Jurassic upwards, after Moscariello (2019). The Malm and the Lower Cretaceous are both potential geothermal reservoirs in the basin. In this study, we focus on the Lower Cretaceous (marked with yellow star). C) Cross section showing the NW-verging Alpine thrusts that separate the target reservoir (black box) from the analogue outcrops. Modified after Bellahsen et al. (2014); Moscariello (2019); Kalifi et al. (2021); Marro et al. (2023)

(e.g. Lacombe et al., 2011; Sanderson et al., 2024). A theoretically complete discontinuity association (DA) consists of four sets of discontinuities: one ~~mode-I~~ opening-mode set, oriented perpendicular to $\sigma 3$; a conjugated pair of ~~mode-II fracturesor vein arrays~~shear fractures, with a ~~~~60° to 30° angle respectively, bisected by $\sigma 1$; and a stylolite forming perpendicular to $\sigma 1$. In ~~this study~~ the study area, many fractures contain mineral deposits, and are then termed as veins. They are mainly found in arrays, ~~mode-I and mode-II discontinuities in general are referred to as fractures . If a fracture is (partially) filled with cement, they are called veins. Veins are treated similarly as other fractures for determining DAs. In the study area, they are found as mode-I opening fractures, mode-II shear fractures, and vein arrays~~belonging to semi-ductile shear zones ~~. The latter~~ that may form conjugate pairs similar to ~~mode-II fractures (Beach, 1975).~~ shear fractures fractures (Beach, 1975). As the aperture and infill of fractures in the outcrop do not necessarily coincide with subsurface (see e.g. Bauer et al., 2017), we use veins in the same way as other fractures to define DAs in the field. The consequences of this approach will be later discussed.

~~Observations in the field are made~~ DAs are documented in the field per station with a size of ~~~~10x10 meters. We aimed to distribute the stations as evenly as possible over the studied area in order to obtain a representative dataset, but the quality of the outcrop exposure also affected the choice of the locations (Peacock et al., 2019)~~around ten squared meters. Discontinuities that are compatible in a single stress field are thus observed in close vicinity of each other. In each station, we document the discontinuities that can be placed into a DA. The orientation of the DAs are used to map the related paleostress directions. To ensure the robustness of the reconstructed paleostress directions, we consider a minimum of two discontinuity sets that are associated together to define a DA. For example, a stylolite together with a conjugate pair of ~~mode-II~~ shear fractures is considered a very reliable indicator. On the contrary, we discard ~~isolated~~ features which provide ambiguous stress information, such as isolated ~~mode-I~~ opening fractures.

This method inherently means that not all discontinuities observed are documented. To quantify how representative the defined associations are for the total network, we measured augmented circular scanlines on ~~7 pavements (Mauldon et al., 2001; Watkins et al. . As the Parmelan is the only outcrop providing quality pavements to conduct circular scanline analysis, all scanlines are taken there~~seven pavements on the Parmelan (Mauldon et al., 2001; Watkins et al., 2015a). Per pavement, a total of ~~4 to 12~~ four to twelve scanlines with a radius of ~~1~~ one meter are collected. The orientation and type of discontinuities that intersect the circular scanlines are documented. The qualitatively defined associations from the nearest by station are used to separate the loose features that cannot be understood in the framework of an association from those that do. This gives an indication of the portion of discontinuities that fit within the framework of associations with respect to the total network.

3.2 DAs in outcrop as prediction for the ~~link between outcrop and~~ subsurface

The mapped paleo principals stresses per station are used to determine the stress regime in which the DA was formed (i.e. normal, reverse, or strike-slip). We assume that all DAs are formed in Andersonian stress fields (Anderson, 1905), i.e. two of the principal stresses were positioned horizontally at the timing of discontinuity formation. This is used to reconstruct the relative timing between the formation of a DA and the tilting of the strata (figure 2). If two of the three principle paleostresses are oriented parallel to the bedding, and the bedding is tilted, we infer that the DA formed prior to the tilting of the strata.

~~The relative timing between different DAs is reconstructed based on abutment and cross-cutting relationships of individual discontinuities.~~

~~In our research area, up to 3 different DAs are~~ Multiple DAs can be observed in a single station (in this study, we document a maximum of three). If the difference between the stress fields of two different DAs is only a permutation of the principle stresses, the simplest cause is a change in overburden (Bertotti et al., 2017) or by intermediate stress regimes (Simpson, 1997), rather than a different tectonic event. Therefore, these DAs are grouped into single events.

We use two criteria to define regional, background network forming events. Firstly, the relative timing of the DAs that make up the event must be prior to tilting of the strata. Secondly, the orientation of the principle stresses of the DA must be similar in all analogue outcrops that surround the target reservoir, i.e. constant on a regional scale. If the two criteria are fulfilled, we predict that the target reservoir that is located between the analogue outcrops, also is affected by these regional events. ~~The regional events we use to predict the orientation of discontinuities in the subsurface, and we use~~ We use this prediction to ~~improve the understanding of the fractures~~ separate the background-related discontinuities observed on BHI ~~from drilled in the target reservoir by separating the background-related discontinuities from the total network~~of the two wells that penetrate the target reservoir, namely GEo-01 and GEo-02.

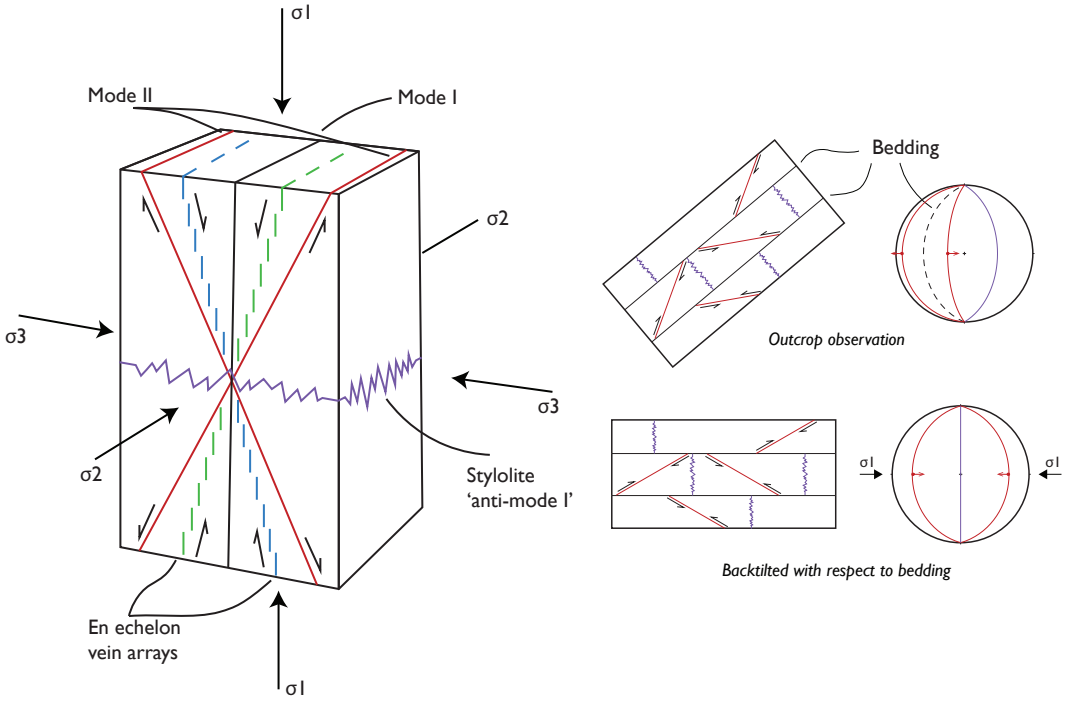

Figure 2. Left: Conceptual model illustrating a discontinuity association, adapted from Hancock (1985). There are four discontinuity sets that can form coeval in a single stress field, and are therefore in association with each other. For ~~legenda~~ legend of colours, see figure 3. Right: illustration of how the timing of the formation with respect to tilting of the bedding is deduced. After back-tilting the association with respect to the bedding, the maximum principal stress becomes horizontal. Therefore, all the discontinuities that make the set (in this case, a conjugate pair of shear fractures and a stylolite), formed prior to tilting of the strata and are thus part of the background network.

4 Geological Background

The Geneva Basin is located in the western part of the Swiss Molasse Basin/North Alpine Foreland Basin (figure 1). It is bounded by the Jura Mountains in the northwest, the Salève Range in the southeast and the Vuache range in the southwest. In the subsurface of the basin, the Mesozoic strata are dipping 10° to 20° to the southeast. The depth of the top of the Lower Cretaceous increases from surface exposures in the northwest (Jura Mountains) to ~1400 m in the southeast at the foot of the Salève Range (Jenny et al., 1995; Guglielmetti et al., 2020).

At present-day, exposures of the Lower Cretaceous are found in the mountain ranges surrounding the Geneva Basin and the Bornes Massif, part of the Sub-Alpine Chain (figure 1). In the Bornes Massif, the Parmelan plateau contains excellent exposures of the Lower Cretaceous carbonates. The plateau of the Parmelan is located in the crest of a box-fold (Berio et al., 2021), underlain by a NW-vergent thrust (Bellahsen et al., 2014) that structurally separates it from the Salève Range in the northwest. The Salève Range is also positioned above a NW-vergent thrust that marks the southeastern boundary of the Geneva Basin (Charollais et al., 2023). The Lower Cretaceous is exposed on the SE-dipping limb of this range. On the other side of the Geneva basin, the Jura Mountains contains several Lower Cretaceous exposures. The mountain range is shaped by NW-verging folds and thrust formed by thin-skinned deformation (Homberg et al., 2002; Sommaruga et al., 2017). The Vuache Fault is part of a system of sinistral strike-slip faults related to the NW-vergent thrusting in the Jura (Homberg et al., 2002; Smeraglia et al., 2022) . Transpression along this fault gave rise to the Vuache Range, with several exposures of the Lower Cretaceous carbonates.

The Lower Cretaceous formations consists predominantly of carbonates, with intercalations of marl layers (Rusillon, 2017; Strasser et al. . They are deposited in a branch of the Tethys Ocean (Clavel et al., 2007, 2013). Subsequently, they are buried beneath Eocene to Pliocene molasse sediments in the foredeep of the Alpine Orogeny, whose thickness tapers towards the northwest. The estimated maximal burial depths of the Lower Cretaceous range between 2000 m in the Geneva Basin (Schegg and Leu, 1998) and 4000 m in the Bornes Massif (Butler, 1991; Moss, 1992; Deville and Sassi, 2006). In the Early Miocene, shortening in the Western Alps was accommodated by different folds and thrusts with a northwest vergence (Kalifi et al., 2021; Marro et al., 2023) , ultimately leading to the exhumation of the Lower Cretaceous in the present-day mountain ranges in the Pliocene (Cederbom et al., 2004) .

A) Simplified geological map modified after the 1:200.000 geological map of the Swiss Federal Office of Topography. The Geneva Basin (dashed black line) is located at the most western termination of the North Alpine Foreland Basin. Analogue outcrops of the Lower Cretaceous target reservoir are found in the Jura, Vuache, Salève and Bornes Massif (Parmelan) mountain ranges. Coordinates in UTM 32N reference frame. B) Synthetic log of the sedimentary succesion in the Geneva Basin, from the Upper Jurassic upwards, after Moscariello (2019). The Malm and the Lower Cretaceous are both potential geothermal reservoirs in the basin. In this study, we focus on the Lower Cretaceous. C) Cross section showing the NW-verging Alpine thrusts that separate the target reservoir (black box) from the analogue outcrops. Modified after Bellahsen et al. (2014); Moscariello (2019);

4 Results

We documented DAs at 28 different stations in the study area. ~~The first area we will describe is the plateau of the Parmelan, part of the Bornes Massif.~~ Due to the ~~superb quality of this exposure~~ quality of the exposure on the Parmelan, the majority (18) of the stations are documented there~~. In total there are three different associations observed on the Parmelan~~, with a total of three different DAs. The stations in the Jura and Vuache are described together (9 in total). In these outcrops, a total of four different associations are defined. The third area is the Salève Range. Due to limited exposures on top of this range, only one station is recorded here, where one association is defined. All the defined associations can ultimately be grouped into two regional discontinuity forming events that formed pre-tilting of the strata.

4.1 Parmelan

Veins, stylolites and shear fractures are common on the Parmelan and can be arranged in discontinuity associations. The oldest association (PA1) is expressed by a conjugate pair of shear fractures and tectonic stylolites, observed on meter-scale. The shear fractures strike ∼045°-225° with a low dip angle with respect to the bedding (∼15°-30°). Dissolution on the shear planes makes them clearly visible on bed-perpendicular exposures (figure 3A). In some instances, slickensides are preserved on the shear planes, indicating reverse kinematics. The tectonic stylolites have a similar strike as the shear fractures, but are bed-perpendicular. The angular relationship between the shear fractures, stylolites and bedding are observed everywhere, even in the steeply dipping limbs of the box fold that shapes the Parmelan (e.g. station 18). Therefore, they are formed prior to the tilting of the strata. This association formed in a reverse stress regime with $\sigma 1$ oriented NW-SE.

The second association (PA2) comprises both small and large discontinuities, ranging from meter to kilometer in length. The smaller discontinuities are made up of two sets of sub-vertical vein arrays with opposing sense of shear (figure 3B) and tectonic stylolites. The latter similarly oriented as those of PA1. Sinistral arrays have an average strike of 150°-330°, whereas dextral arrays strike 120°-300° on average. The cement of the veins is yellow-white and have a blocky texture.

On a large scale, the plateau is dissected by two sets of fractures with similar orientation as the vein arrays (figure 4). They range in length from 100 to 3000 m. In the field, they appear as narrow bundles ($<$1 m) of smaller sub-vertical fractures. Dissolution along these fractures has created a karst system that is connected to an extensive cave system below the plateau (Lismonde, 1983; Masson, 1985). On the plateau, there are no offset markers that indicate horizontal displacement along these structures and no kinematic indicators are observed. At the northern edge of the plateau however, in front of the entrance to the Diau cave (see figure 10 for location), these fractures intersect a vertical cliff, and here bed-parallel slickensides on the fracture planes are preserved. The shear fractures form a conjugate pair, so their structural attitude is similar to the vein arrays on top of the plateau, and are thus grouped into PA2. The associated stress regime of PA2 is a strike-slip regime, with $\sigma 1$ oriented NW-SE. This is similar to PA1, with the only change being a permutation of $\sigma 2$ and $\sigma 3$. Therefore, PA1 and PA2 together are considered as part of one event.

The third association (PA3) is also made up of a conjugated pair of sub-vertical vein arrays and tectonic stylolites, but with different orientations than those of PA2 (figure 3C). The dextral vein arrays strike ∼080°-260° and the sinistral arrays strike

∼120°-300°, with the cement of the veins being grey-coloured. The length of the discontinuities range from cm to 10s of meters. The stylolites are bed-perpendicular and strike ∼170°-350°. The veins that form the arrays occasionally cross-cut and displace those of PA2 (figure 3D), and are therefore interpreted as being younger in age. The paleostress regime related to this association is strike-slip, with $\sigma 1$ oriented ∼W-E.

To investigate how representative the above described associations are for the total network present on the Parmelan, we measured augmented circular scanlines on 7 different pavements on the Parmelan (see figure4 for location). Up to 75% of the total discontinuities observed can be understood within the framework of the predefined associations, and the majority belong to PA3 5. The percentages vary per pavement investigated, illustrating the spatial variability of the background network.

4.2 Jura and Vuache

Four different associations have been documented in the Jura and Vuache. In all cases, they formed prior to tilting of the strata. The first association (JA1) comprises a conjugate pair of shear fractures with a low-angle with respect to the bedding and bed-perpendicular, tectonic stylolites (figure 6A). The strike of the shear fractures and stylolites is ∼035°-215°. Slickensides on the shear planes indicate reverse kinematics. The reconstructed $\sigma 1$ of JA1 is oriented NW-SE.

The second association (JA2) is made up of a conjugated pair of bed-perpendicular shear fractures (figure 6B), together with tectonic stylolites. Sinistral fractures strike ∼170°-350°, dextral fractures strike ∼110°-290°. Slickensides on the shear planes are always parallel the bedding. Tectonic stylolites strike of ∼035°-215°, similarly as those of JA1. The stress regime of JA2 is strike-slip, with $\sigma 1$ oriented NW-SE. The difference between JA1 and JA2 is a premutation of $\sigma 2$ and $\sigma 3$. Therefore, they are grouped into a single event.

The third association (JA3) is ~~comprised~~ composed of ∼000°-180° striking reverse shear fractures with a low angle with respect to the bedding (figure 6C), and bed-perpendicular tectonic stylolites. They formed in a reverse stress regime with $\sigma 1$ oriented W-E.

The fourth association (JA4)is expressed by bed-perpendicular ∼140°-320° striking sinistral shear fractures and ∼075°-255° striking dextral shear fractures (figure 6D), together with ∼010°-100° striking bed-perpendicular stylolites. This association is indicative of a strike-slip regime with $\sigma 1$ oriented W-E. This orientation is the same as JA3, and therefore they are part of the same event.

4.3 Salève

In the Salève, only one (SA1) is documented. Shear fractures that strike ∼030°-210° and have a low angle with respect to the bedding (figure 7) are associated together with ∼035°-215° striking bed-perpendicular stylolites. The related stress field is a reverse regime with $\sigma 1$ oriented NW-SE.

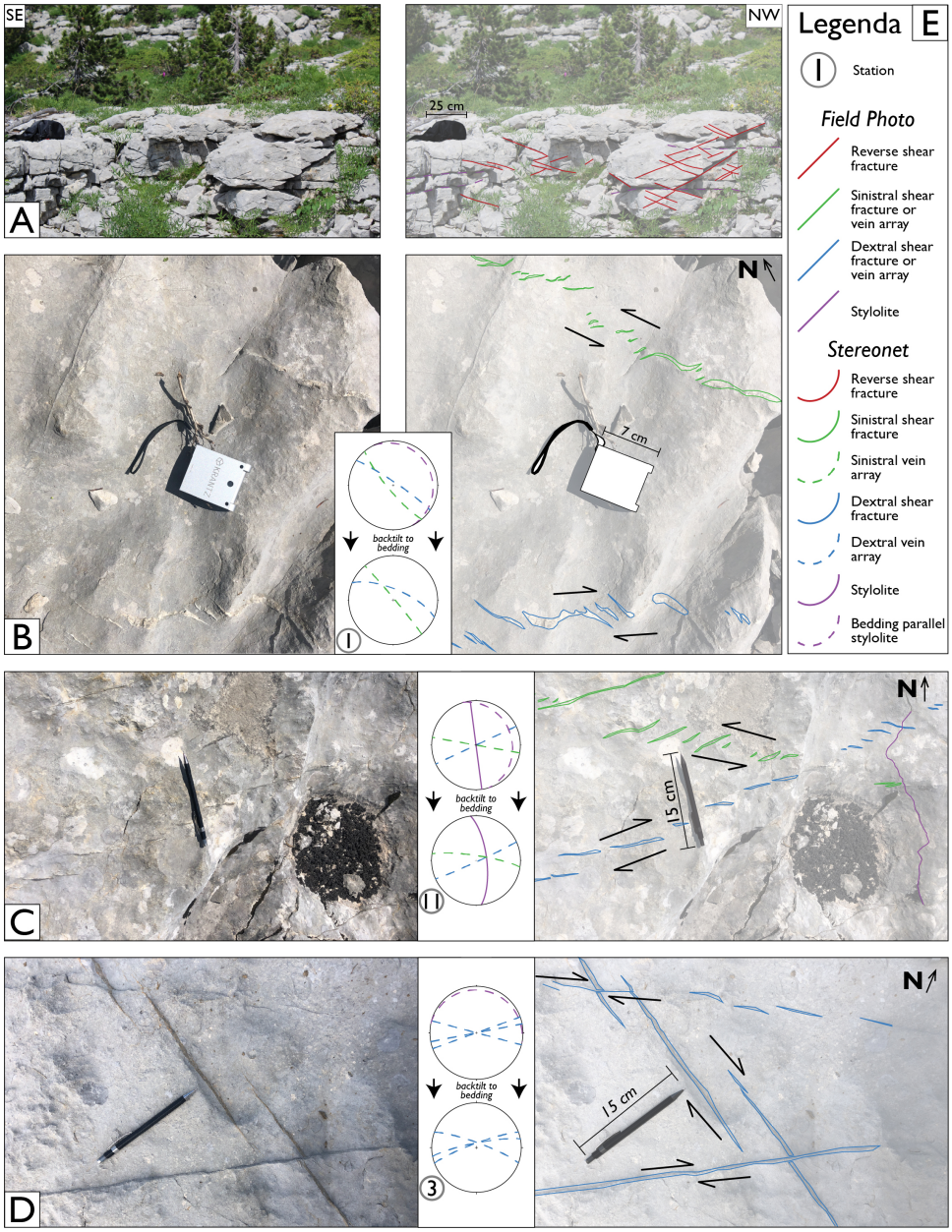

Figure 3. Field examples of DAs on the Parmelan. A) Low-angle conjugate pair of shear fractures (PA1) with minimal displacement. Dissolution along the shear planes make them clearly visible on bed-perpendicular exposures. B) Top view image of a conjugate pair of vein arrays of PA2. C) Top view image of PA3 conjugate pair of vein arrays in association with a bed-perpendicular stylolite. D) Dextral vein array of PA3 crosscuts and slightly displaces a dextral vein array of PA2, indicating the relative timing of formation of the two associations. All stereonets, here in and in following figures, are lower hemisphere projections. E) ~~Legenda~~ legend for the colours used on the intepretation of the photographs and stereonets.

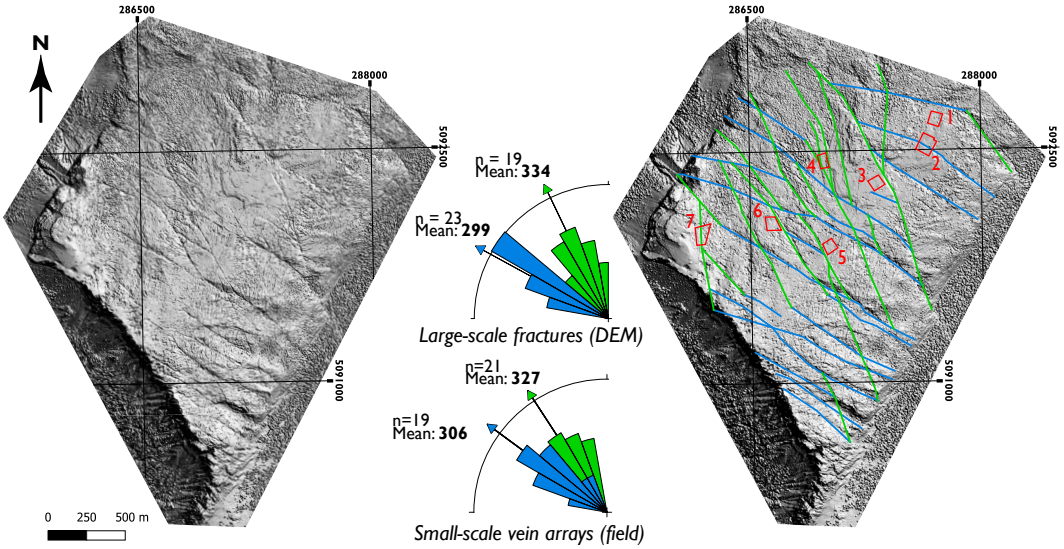

Figure 4. Digital elevation model of the Parmelan derived from LiDAR HD survey of IGN. The large-scale fracture network on the plateau is clearly visualized. The two main orientation of this network (upper rose diagram) correspond well with the orientations of the vein arrays of PA2 (lower rose diagram). At the northern plateau, opposing sense of shear is observed on these fractures, and therefore they are also grouped into PA2. The red insets refer to the pavements where circular scanlines are taken (see Table 1 for the results of the scanlines). Pavement 2 is shown as example in figure 5. For the colour code of the traced fractures, see ~~legenda~~ legend of figure 3E.

4.4 Regional discontinuity-forming events

Based on the orientation of $\sigma 1$ of the associations in the different studied areas, we can define two regional discontinuity formation events (figure 9). The first event (E1) is characterized by a NW-SE trending, sub-horizontal $\sigma 1$. This orientation of $\sigma 1$ is both recorded by the reverse associations (PA1, JA1 & SA1) as well as by strike-slip associations (PA2 & JA2). In all outcrops, the reverse regime is similarly expressed by low-angle conjugate pairs of shear fractures. Bed-perpendicular vein arrays of the strike-slip association are also observed in the Parmelan, Jura and Vuache. On top of this, in the Jura and Vuache, the strike-slip association is also expressed by conjugated brittle, sub-vertical shear fractures.

The second event (E2) is also made up of a reverse and strike-slip association, but with a sub-horizontal $\sigma 1$ oriented $\sim$W-E (figure9). In the Parmelan, only the strike-slip association is documented in the form of vein arrays and bed-perpendicular stylolites (PA3). In the Jura and Vuache, there is also a reverse association documented (JA3) with similar $\sigma 1$ as a strike-slip association (JA4). The latter is mainly depicted by bed-perpendicular shear fractures, and less so by vein arrays, in contrast to the Parmelan.

A pre-tilting relative timing for E1 and E2 is observed in all studied areas. This implies that E1 and E2 were formed prior to Alpine fold-and-thrusting, and thus form the background network. As these events are consistently observed on all sides of the Geneva Basin where the target reservoir is located, we predict the presence of this background network in the subsurface as well.

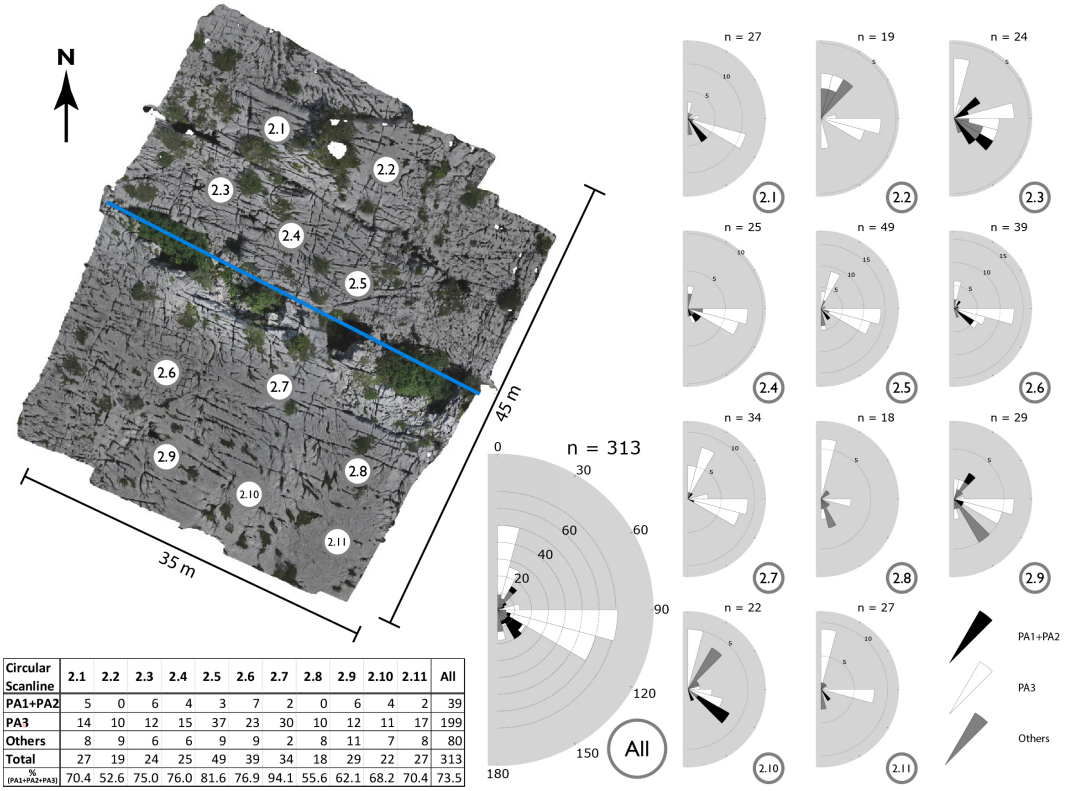

Circular Scanline	2.1	2.2	2.3	2.4	2.5	2.6	2.7	2.8	2.9	2.10	2.11	All
PA1+PA2	5	0	6	4	3	7	2	0	6	4	2	39
PA3	14	10	12	15	37	23	30	10	12	11	17	199
Others	8	9	6	6	9	9	2	8	11	7	8	80
Total	27	19	24	25	49	39	34	18	29	22	27	313
% (PA1+PA2+PA3)	70.4	52.6	75.0	76.0	81.6	76.9	94.1	55.6	62.1	68.2	70.4	73.5

Figure 5. UAV-derived orthorectified image of a pavement on the Parmelan (for location, see figure 4). Augmented circular scanlines with 1m radius show that the majority (75 %) of the observed discontinuities are in line with the qualitatively defined associations in station 4 (for location, see figure 10, for definition DAs, see figure 8). The scanlines are taken on both sides of a large-scale ENE-WSW fracture (blue line, see figure 4). There is no significant change in intensity of the discontinuities closer this fracture, suggesting that the large-scale fracture does not control the geometry of the total discontinuity network.

Table 1. Results of the augmented circular scanlines measured on the Parmelan. See figure 4 for the locations of the pavements. Results of circular scanlines of pavement 2 are illustrated in figure 5.

Pavement	No. of Scanlines (1m radius)	Total discontinuities	PA1 + PA2	PA3	Percentage of total
1	9	276	4	79	30.1%
2	11	313	39	191	73.5%
3	12	207	32	110	68.6%
4	6	85	8	39	55.3%
5	9	308	31	84	37.3%
6	4	150	5	79	56.0%
7	4	126	17	70	69.0%

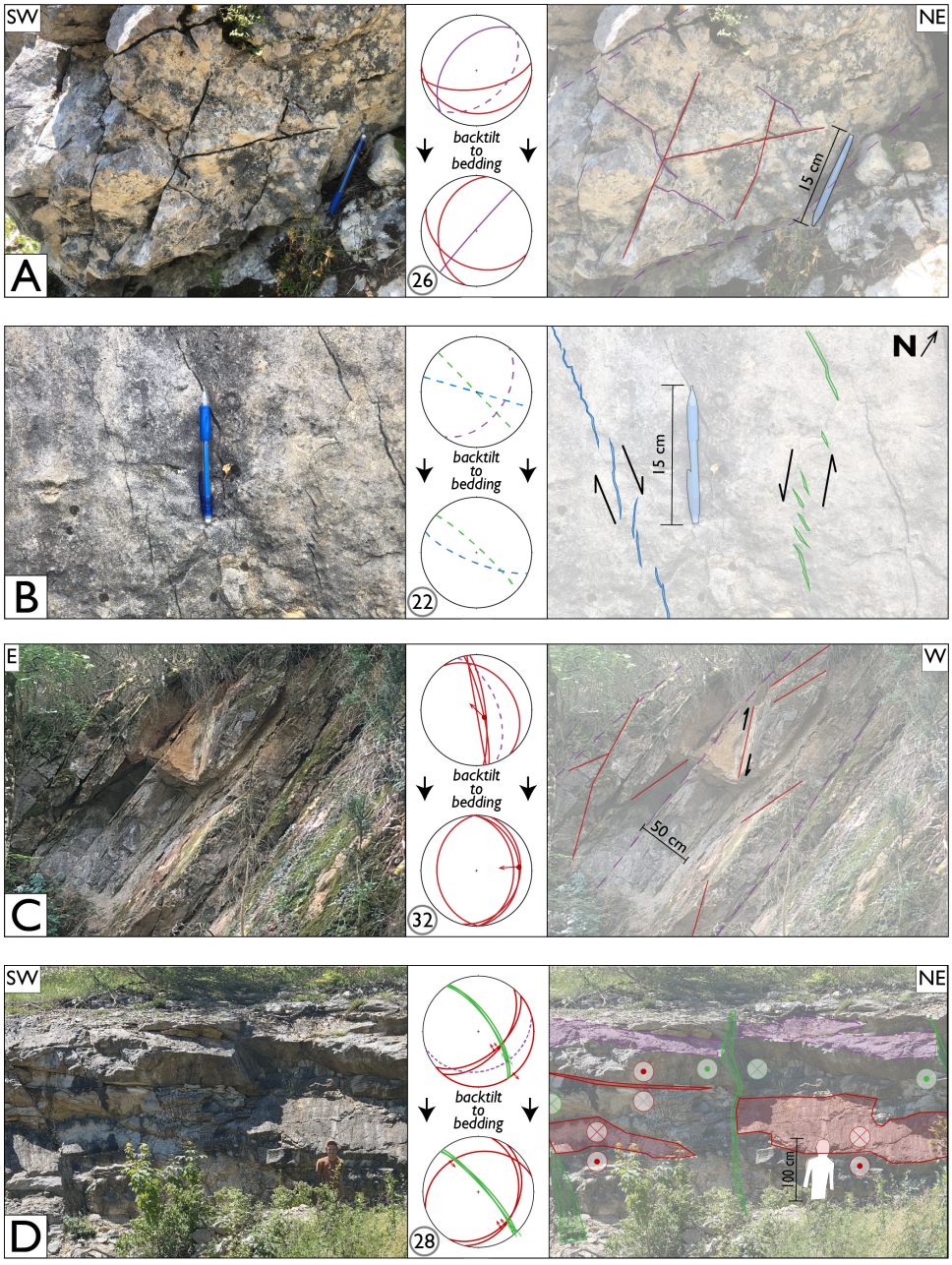

Figure 6. Field examples from the Jura. A Reverse shear fractures with low angle with respect to the bedding, in association with a bed-perpendicular stylolite together form the reverse association JA1. B Top view of a bedding surface displaying a conjugate pair of vein arrays. Together with similarly oriented bed-perpendicular shear fractures they form a strike-slip association JA2. C Tilted shear fractures at low angle with respect to the bedding. The strike after backtilting is ∼N-S. They form the reverse association JA3. D Reverse fractures of JA1 are cross-cut by bed-perpendicular, sinistral shear fractures of JA4. The plunge of the slickensides on these shear fractures indicates they formed prior to tilting of the bedding. For ~~legenda~~ legend see figure 3E.

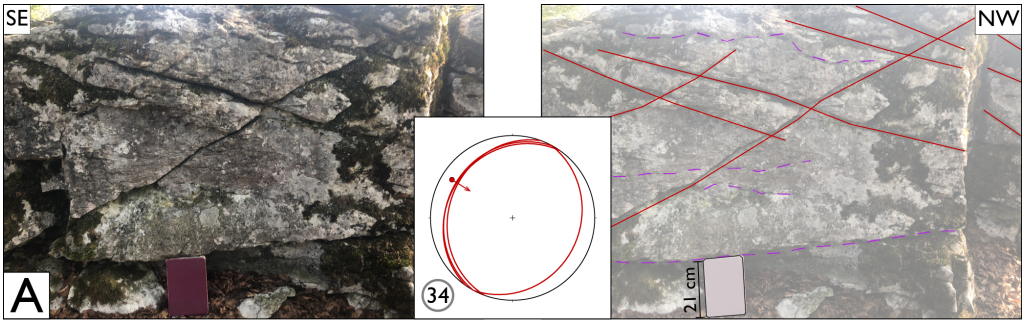

Figure 7. Field example from the Salève. A conjugate pair of reverse shear fractures at low angle with the bedding define the reverse association SA1. For ~~legenda~~ legend see figure 3E.

5 Improving BHI interpretation

5.1 ~~Description of GEo-01 and GEo-02~~Geothermal exploration wells in the Geneva Basin

We use the prediction of the background network in the subsurface of the Geneva Basin based on the analogue outcrops for the interpretation of BHI of two geothermal wells drilled in the basin (GEo-01 and GEo-02, for location see figure 1). The discontinuities of which the orientation fits within the predicted background network are identified in the dataset and subsequently considered as part of the background network. Then, we evaluate the proportion of the background network with respect to all discontinuities observed in the well.

The two investigated wells both penetrate the Lower Cretaceous carbonates, and as there are no cores of the wells, all features are interpreted on the BHI only~~(Doesburg, 2023)~~. In GEo-01, the Lower Cretaceous is observed between 411 m and 533 m (MD). In this well, two types of image logs are acquired for fracture analysis: optical borehole imaging (OBI) and acoustic borehole imaging (ABI). GEo-02 is located 7 km south-southeast of GEo-01 and here the Lower Cretaceous is found at a depth between 770 m to 996 m (MD). For this well, only ABI-logs are available. Feature picking on these logs was carried out with WellCAD (ALT) program software.

The feature picks are divided over 5 different categories~~, following the methodology of Doesburg (2023)~~; bedding, veins, open fractures, induced fractures and unclassified fractures. Bedding planes are defined by their repetitive character and the fact that they cannot cross-cut any other feature. Veins are highly reflective in OBI, whereas open fractures are transmissive. Veins ~~are invisible on ABI and could therefore not be picked on the image logsof~~ were not observed on the ABI logs, either because they are not present, or due to the limited contrast between the host rock and fracture infill. As GEo-02 ~~. If feat~~ only has an ABI-log, no veins are interpreted in this borehole. If features are transmissive in OBI, have an irregular surface and the dip angle is high (>85 degrees) they are classified as induced fractures, although it should be noted that separating induced fractures from natural fractures remains a challenge ~~(?)~~(Lorenz and Cooper, 2017). Features that are both transmissive in OBI and have a low amplitude on the ABI are interpreted as open fractures. Distinguishing mode-I from mode-II is not possible on

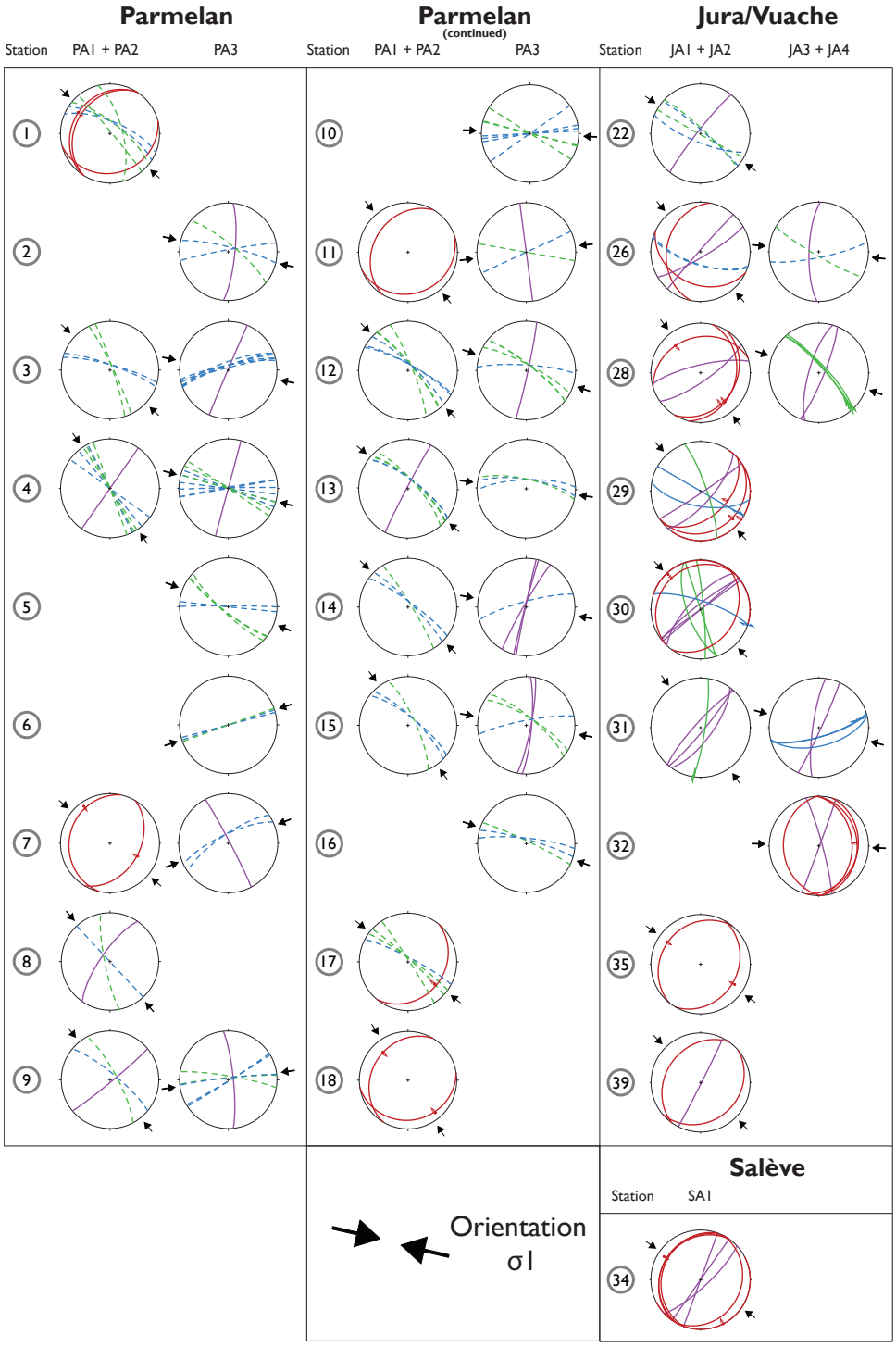

Figure 8. Stereonets of the events documented in all the stations of the analogue outcrops. All data is backtilted with respect to the bedding. The black and white arrows are the inferred orientations of $\sigma 1$ of E1 and E2 respectively, and correspond to the arrows plotted on figure 10. For the ~~legenda~~ legend of the colours, see figure 3

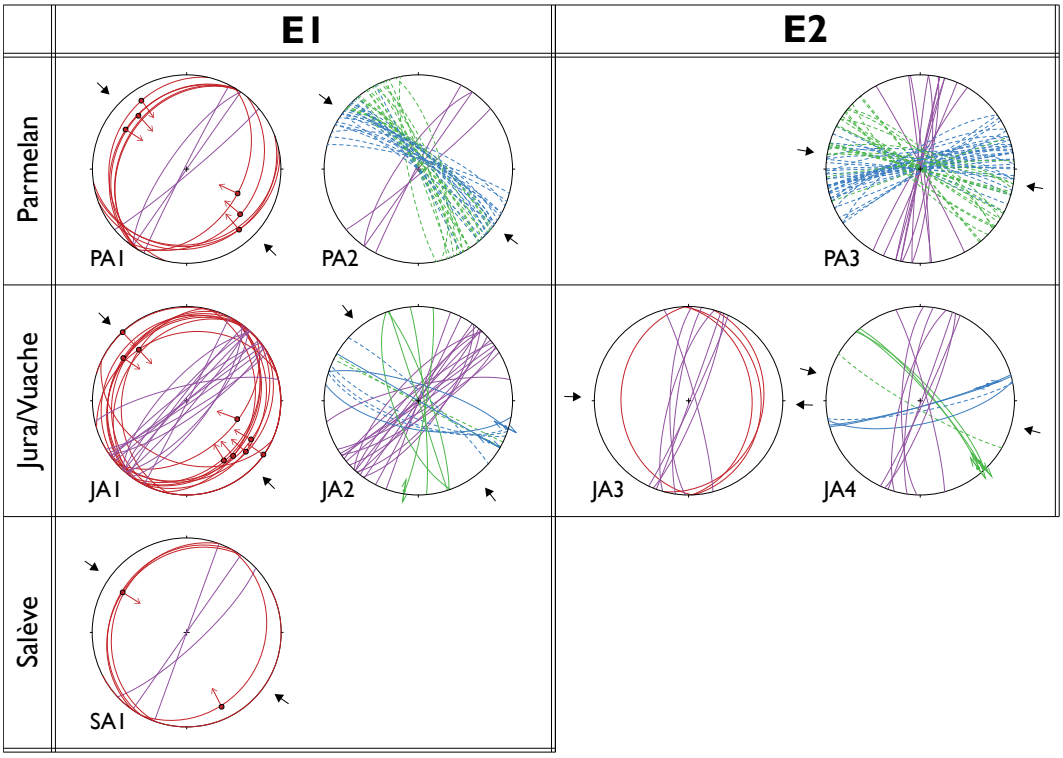

Figure 9. The associations of the different outcrops grouped into regional pre-tilting events, based on the orientation of $\sigma 1$. In all outcrops, a reverse association with $\sigma 1$ oriented ~NW-SE is observed (PA1, JA1, SA1). In the Jura and Parmelan, a strike-slip association (PA2 and JA2) with similarly oriented $\sigma 1$ is documented, and together they are grouped into E1. E2 is predominantly a strike-slip association, complemented by a reverse association in the Jura/Vuache. E2 is not observed in the Salève, presumably due to a lack of exposures. All data is backtilted with respect to the bedding. For ~~legenda~~ legend see figure 3E.

the image logs, so they are not differentiated during the picking of fractures. If a fracture pick did not meet any of the above criteria, it was not classified.

Firstly, the bedding planes are separated from the other interpreted features. In GEo-01, a total of 195 bedding surfaces are identified (figure 11). When plotted against depth, the dip direction of these planes exhibit a clockwise rotation with depth, from north-dipping at the top, gradually transitioning into south-dipping at the bottom. Also, the dip angle varies with depth, with a low angle at the top and bottom, but a gradual increase between 440-480 m (MD) up to 60°, giving an overall bell-shaped curve. In GEo-02, a total of 176 bedding planes are picked (figure 11). In contrast to GEo-01, the dip direction remains constant with a dip towards the ESE and a dip angle between 10-20°.

For the implementation of the prediction based on outcrop work, we only considered the natural fractures (open fractures and veins), and discarded the induced and unclassified picks from the datasets. Then, the total amount of natural fractures observed in GEo-01 is 820, and for GEo-02 is 211. To compare these discontinuities with the outcrop prediction, they were backtilted with respect to the closest bedding measurement on the BHI (figure 12). The backtilted discontinuities are subsequently compared with the predicted background network as defined in the outcrops.

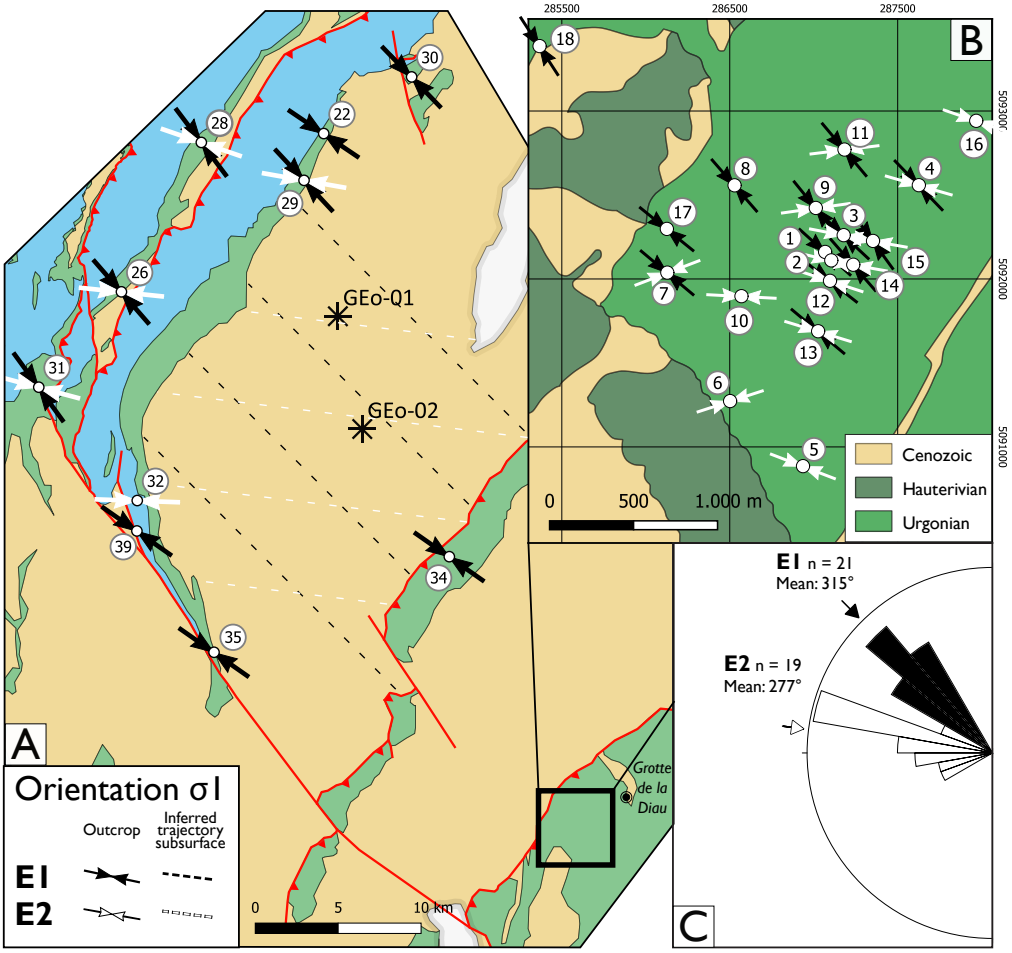

Figure 10. Overview of the mapped orientation of $\sigma 1$ of the regionally defined events E1 and E2 recorded in A) the Jura, Vuache, Salève and B) Parmelan C) Rose diagram of the orientations of $\sigma 1$ showing that there is a $\sim$45° anticlockwise rotation between E1 and E2.

5.2 Comparison with DAs observed in the field

The orientations of the regional events in the outcrop are used to predict the geometry of individual discontinuity sets that make the background network in the subsurface. We consider the average orientation of the principal stresses of the regional events, and define orientations of discontinuity sets related to this orientation. For E1, the orientation of $\sigma 1$ is 135-315° and for E2 it is 097-277° (figure10). For the low angle shear fractures, we assumed a strike perpendicular to $\sigma 1$ with a dip angle of 30 degrees. For the stylolites, the strike is also perpendicular to $\sigma 1$, but with a dip angle of 90 degrees (perpendicular to the bedding). As in the outcrop, the majority of the discontinuities that make up the strike-slip associations are bed-perpendicular vein arrays, we considered a 15 degree angle between $\sigma 1$ and the strike of the vein arrays for the prediction in the well. Lastly, the opening fractures are bed-perpendicular with a strike parallel to $\sigma 1$. The combination of these sets are used to identify the fractures in

the well that fit within this predicted assoications. If a fracture pick on the BHI deviates less than 30° (azimuth + dip) from the predicted orientation of a set, these fractures are considered as part of that discontinuity set (figure 12). This maximum deviation is considered reasonable, as there is some variability in the observed DAs in the outcrop. On top of that, there is a margin of error in the BHI interpretation as well.

For the well GEo-01, 350 discontinuities (44% of total) fit in the associations of E1 and E2, of which 236 are open fractures, and 114 veins. In GEo-02, the total number of discontinuities that fit the predicted associations is 104 (50% of total). As there is no ABI for Geo-02, all the fractures that are identified are open. The contribution of E1 and E2 is about equal. The majority of the discontinuities in the two wells are low-angle shear fractures (175 and 86 for Geo-01 and Geo-02 respectively).

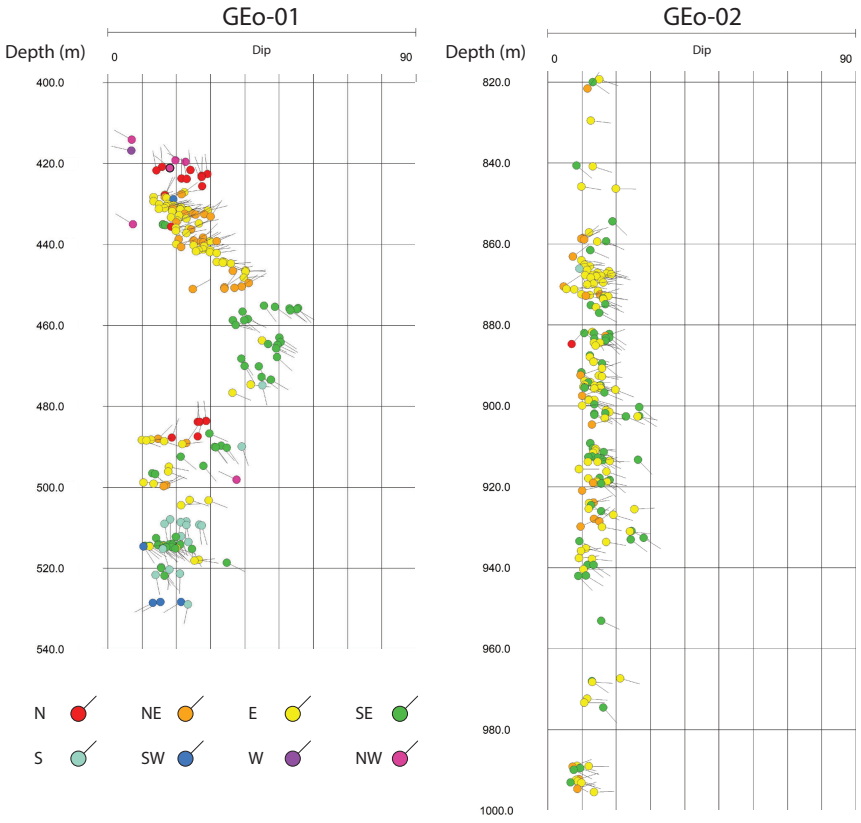

Figure 11. Tadpoles of bedding picks versus depth on GEo-01 and GEo-02 after Doesburg (2023). In GEo-01, there is a variation in both azimuth and dip with depth. The bell-shaped curve suggests the presence of a fold, potentially related to a fault around 480 m depth. This contrasts with GEo-02, where no change is observed in bedding orientation with depth.

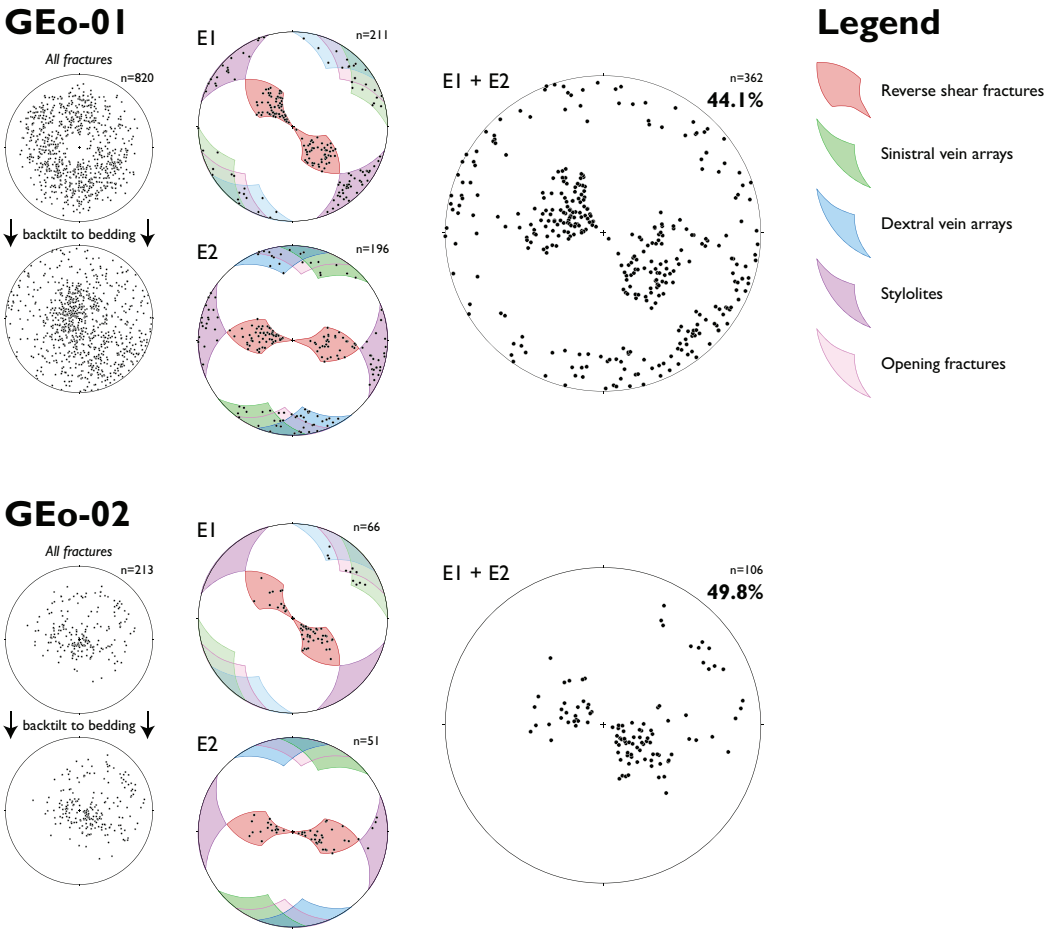

Figure 12. All fractures interpreted from the BHI of GEo-01 and GEo-02 by Doesburg (2023) compared with the predicted associations based on the outcrops. First, the fractures in the well are backtilted with respect to the bedding, as the predicted associations are formed pre-tilting. Then, the fractures that fit in the predicted associations of E1 and E2 are counted. The coloured areas are based on the average orientations of $\sigma 1$ of the two regional events (figure 10C), with a deviation margin of 30° (azimuth + dip). There is a small overlap between some sets of E1 and E2: fractures are not counted double when calculating the total percentage of the predicted fractures.

6 Discussion

6.1 ~~The robustness of DAs~~ DA-method as ~~the analog~~ analogue link

The regional events captured by the method of DAs reveal similar paleostress orientations as previous studies focusing on the deformation history of the Parmelan (Berio et al., 2021) and the Jura and Vuache ranges (Homberg et al., 1999, 2002). In the Parmelan, Berio et al. (2021) define two pre-folding events with a reverse and strike-slip component with an ∼NW-SE orientation of $\sigma 1$, similar to E1. These authors also document a strike-slip event with an ∼E-W oriented $\sigma 1$ identical to E2 but interpret this event to be post-folding (Berio et al., 2021). In the Jura and Vuache ranges, the reverse and strike-slip regimes of E1 are also observed by Homberg et al. (1999). However, the inferred timing of these regimes is different; only the strike-slip component is interpreted as pre-tilting of the strata, whereas the reverse regime is considered syntectonic, because the majority of the observed reverse slip vectors were not pre-folding (Homberg et al., 2002). This is in contrast to our observations of clearly pre-folding shear fractures related to the reverse regime (fig. 6A).

The main difference between the DA method and previous studies is the interpreted timing of discontinuity-forming events, which reflects the specific aim of the methodology proposed in this study. The goal of the DA method is to use the outcrop as an analogue of the subsurface to better predict the geometry ~~and flow efficiency of the fracture~~ of the background discontinuity network present at depth that is not directly observable. ~~On the contrary, the studies of Berio et al. (2022) and Homberg et al. (2002)~~ This is in contrast to the studies of Berio et al. (2021) and Homberg et al. (2002) that focus on the deformation history of the outcrop itself, aiming at retracing the chronological succession of events that created the discontinuities in the outcrop. The consequences of these different approaches are best illustrated with the reverse regime of E1. If this event is linked to folding, it may be expected to produce localized deformations, opposed to the distribution of a background network (Watkins et al., 2015b). However, this event, producing reverse shear fractures, could also be interpreted as having formed during the ~~layer parallel shortening~~ layer-parallel-shortening (LPS) phase before the onset of regional folding. Lacombe et al. (2021) dated the sequence of events shaping a series of folds observed in the Apennines, Pyrenees and in the Rocky Mountains. They found that the LPS-phase largely predates the onset of localized deformations occurring during fold growth and late stage fold tightening. Therefore, the LPS deformation phase is likely to produce the same diffuse fractures observed in the Vuache and the Jura. Considering the E1 regime as localized and restricted to fold structures dramatically changes the prediction of these features in the subsurface. In the absence of folds in the subsurface, these fractures will be overlooked, although they are largely present in the investigated wells in the Geneva basin (see fig 12).

~~In the case of E2, the~~ A key aspect of the DA-method is that it targets to capture regional events to enhance the predictability ~~of the method~~for the subsurface. The interpretation of E2 demonstrates this capability of the DA-method. On the Parmelan itself, there is no direct evidence for the relative timing of E2 with respect to the folding. In the Jura however, shear fractures of E2 are consistently tilted with the bedding (e.g., figure 6C) and thus formed prior to tilting. Therefore, we ~~interpret~~ consider that the simplest interpretation is that E2 ~~as~~ is also part of the background network~~and consequently present~~ , and consequently predict its presence in the subsurface. Absolute dating of the calcite veins that are part of the background network could

potentially ~~resolve the issue of the timing~~ constrain the timing even further, but so far, geochronology studies in the region have only focused on dating fault activity (Smeraglia et al., 2021; Looser et al., 2021).

6.2 ~~DAs as the guideline for BHI interpretations~~Infill and aperture of discontinuities

~~Boreholes are the only way to sample and characterise the sub-seismic scale discontinuity~~ The DA-method can be used to predict the geometry of the background network in the ~~subsurface of the Geneva Basin. Many data collection methods of faults and fractures are prone to subjective bias, both in the subsurface (Bond et al., 2007) and in outcrops (Andrews et al., 2019; Peacock et al., 20~~ target reservoir, but is limited in extrapolating the aperture and mineral infill of fractures. The geometry is useful when considering stimulating the reservoir, as even the sealed discontinuities may create a strength anisotropy that will control the orientation and propagation of hydraulic fractures (Cao and Sharma, 2022; Rysak et al., 2022). However, for predicting flow behaviour in the reservoir caused by natural discontinuities, modeling the aperture and mineral infill of discontinuities is crucial, as only (partially) open discontinuities might contribute to the flow. At the same time, outcrops should be treated with care when extrapolating these properties to the subsurface (e.g. Bauer et al., 2017; Peacock et al., 2022), also when the link between outcrop and subsurface is established with the DA-method. The timing of fracturing, emplacement of the ~~influence of bias on BHI interpretations has rarely been investigated (Zarian and Dymmock, 2010). The reproducibility of BHI interpretation remains a major challenge, leading to discrepancies in fracture frequency analysis and inconsistent fracture orientation among different interpreters. These uncertainties have a large impact on the characterization of the fracture network and~~ infill and potential dissolution are important factors to consider when extrapolating these characteristics to the subsurface. On the Parmelan, for example, many small-scale (<10 meter) fractures of E1 and E2 are calcite filled (e.g. see figure 3). The diagenetic evolution can be used to constrain the timing of calcite cement formation in the outcrop (e.g. Lavenu and Lamarche, 2018; La Bruna et al., 2 , and subsequently provide insights how the aperture of these discontinuities can be modeled in the ~~population of fracture models of the reservoir. For instance, Tutuarima et al. (2023) studied the BHI of a deep exploration well targeting the geothermal Triassic sandstone reservoirs in the West Netherlands Basin. Over 900 fractures picked; these authors identified that only 32 % of them are natural. Before this work, two consultancy companies studied the same interval, picked roughly the same number of features, and interpreted either~~ subsurface (Elliott et al., 2025). On the other hand, the large-scale fractures (> 100 ~~% or as low as 2.8% as being natural fractures. This discrepancy has large implications for whether considering the targeted reservoir as naturally fractured and therefore suitable for geothermal resource exploitation.~~

~~To reduce biases in fracture interpretation, Andrews et al. (2019) propose to develop a clear sampling strategy before the actual interpretation. The robust analogy between outcrops and the subsurface provided by the DA-method presented in this paper has the potential to create such a strategy for BHI interpretations and , in this way, reduce the impact of bias. The two events that shape the predicted background network~~ m) of E1 on the plateau are currently conductive due to dissolution and karstification (see figure 4). It depends on the timing of fracturing and subsequent dissolution if the conductivity of these fractures can be used as an analogue for the paleokarst network that is observed on top of the Lower Cretaceous in the subsurface of the Geneva Basin ~~are composed of discontinuity sets with a known range of orientations. An adequate fracture picking strategy in the BHI could be to temporarily discard all features that fall significantly outside this predefined range. The~~

resulting picking will therefore focus on isolating the background network from more recent structural objects. After this, the impact of the background network on the flow behaviour of the reservoir can be assessed (see Sect. 6.4). (Eruteya et al., 2024). If E1 was formed prior to sub-aerial exposure of the Lower Cretaceous during the Paleogene, it is likely that they partially controlled the orientation of karst development. On the contrary, if the karstification on the Parmelan only occurred after the exhumation in the Pliocene, similarly dissolved fractures cannot be expected in the subsurface. So, in order to predict the aperture and if discontinuities are sealed in the reservoir, solely based on outcrops, the timing of fracturing and the diagenetic evolution of the formation are both essential to predict which discontinuity sets in the subsurface are likely to be conductive. Another possibility is to use borehole data to assess which discontinuities are conductive, and the DA-method can be part of the workflow to improve the interpretation.

DAs also improve BHI interpretation by predicting the discontinuity type of identified features. Genter et al. (1997) and Fernández-Ibáñez et al. (2018) integrated cores with image logs to improve the subsurface fracture characterization. Both studies show that the correlation with the core is essential for assigning

6.3 DAs improve fracture interpretations of BHI

Borehole images are a practical, widely used, and relatively inexpensive way to sample and characterize the sub-seismic scale discontinuity network in the subsurface. However, there are two main drawbacks to this type of data. Firstly, core-to-log correlations have shown that image logs only are not suitable for characterizing the type of discontinuity to the BHI interpretation. However, cores are expensive to drill, and therefore, often only BHIs are available for subsurface fracture characterization. The discontinuity fracture (e.g. Laubach et al., 1988; Genter et al., 1997; Fernández-Ibáñez et al., 2018). Secondly, image log interpretations are prone to subjective bias of the interpreter (Zarian and Dymmock, 2010), similarly as has been demonstrated for fault interpretation in seismic data (Bond et al., 2007) and fracture data collection in outcrops (Andrews et al., 2019; Peacock et al., 2019).

DAs can complement BHI interpretation by providing the discontinuity type of identified background features. Typically, discontinuity sets defined on the BHI are then BHI (in particular when cores are not available) are all considered as barren or Mode-I opening-mode fractures. Based on this assumption, a classical workflow consists of defining fracture sets, extracting statistical distributions for these sets, and stochastically extrapolating these distributions at the reservoir scale in a discrete fracture network model (Hosseinzadeh et al., 2023).

(e.g. Hosseinzadeh et al., 2023). However, the type of discontinuity will impact the evaluation of the flow behaviour of the network in different ways. Bruna et al. (2019) multiple ways. Several studies have demonstrated that stylolites can be either flow conductive or form flow barriers and could potentially induce compartmentalisation compartmentalization in subsurface reservoirs (Heap et al., 2014; Koehn et al., 2016). Hooker et al. (2012) and Lander and Laubach (2015) showed that Mode-I opening fractures are good flow conductors if cement bridges create a natural propping mechanism in the fracture. Finally, Bisdom et al. (2016) emphasised that the roughness of a fracture discontinuity, which is related to the type, has an impact on its capacity to be reactivated under present-day stress field, which in turn influences its hydraulic aperture under reservoir conditions (Bisdom et al., 2016). These authors also add that typically, Mode-II shear fractures have a higher roughness than

Mode-I opening fractures, therefore highlighting the importance of being able to constrain fracture type at depthin the reservoir. The DA-methodology provides a prediction of the discontinuity type in the borehole, even when the resolution of the BHI is too low to determine this. , and there is no core available to correlate the BHI with.

To reduce biases in fracture interpretation, Andrews et al. (2019) propose to develop a clear sampling strategy before the actual interpretation. In the Geneva Basin, the two events that shape the predicted background network are composed of discontinuity sets with a known range of orientations, based on outcrop work. An adequate fracture picking strategy in the BHI could be to temporarily discard all features that fall significantly outside this predefined range. The resulting picking will therefore focus on isolating the background network from more recent features. This information can be considered during fracture modeling and subsequent flow simulations. After this, the impact of the background network on the flow behaviour of the reservoir can be assessed.

6.4 ~~Impact on fracture modeling and geothermal exploration~~

6.4 Impact on fracture modeling for geothermal exploration

~~Isolating the background network from the total network will improve fracture modeling because the structural driving mechanism that shapes~~ The tectonic driver of the background network is fundamentally different ~~than other parts of the total network~~from the rest of the network, and therefore isolating the background network in the reservoir will improve fracture modeling on reservoir scale. Maerten et al. (2016) developed a method that links discontinuities observed in the well with seismic-scale faults. A given number of random far-field stress states are simulated around the faults, and the perturbation of the stress directions around the faults is calculated. For each simulated stress state, the number of small-scale discontinuities whose orientation fits within the modeled stress field is counted (goodness of fit). The stress state with the highest number of fitting discontinuities is considered the best stress regime, and the discontinuities falling outside this model are discarded from the dataset. The input data for these models are generally all the fractures interpreted from wells. ~~If~~ , or, in other words, it is assumed that all subsurface fractures are fault-related. Instead, we propose to first isolate the background network~~is not isolated from fractures related to more localized deformations (e.g., faults),~~ , as these discontinuities should be extrapolated to the entire reservoir. Only after this separation, the goodness of fit ~~will be affected by the very different mechanisms that these contrasted fracture populations experienced.~~ of fault-related discontinuities should be considered. In this way, the geological understanding of discontinuity formation is better incorporated in the fracture modeling in the reservoir.

~~Besides integrating more geology into the process of modeling fracture networks, the DA method has implications for upscaling~~Another way how the DA method can improve fracture modeling in the reservoir is in the up-scaling strategy. Berre et al. (2019) advocated for mixing explicit and implicit representation of fractures in the model as an effective up-scaling method~~to balance~~ , as it balances the accuracy of ~~up-scaling~~ the process, whilst preserving the geometrical complexity of the network. Typically, the selection criterion between implicit and explicit representation is the length of the fractures (Lee et al., 2001). ~~In addition~~ As an alternative to this method, we propose to use the genetic origin of the fracture as a second criterion. ~~The~~ Due to its regional character, the background network is very suitable for up-scaling strategies~~, due to its regional character, in~~

contrast to the discontinuities formed by local drivers. Here, we will investigate when it is possible to up-scale the background network as a matrix property on the reservoir scale.

The first step is to evaluate the importance . By assessing the impact of the background network on the effective permeability k_{eff} of the reservoir . Numerical work has suggested that there is a relationship between fracture density P_{21} and effective permeability k_{eff} of a fractured medium (Agbaje et al., 2023), so a first-order approximation is to consider the fracture density P_{21} of the background network. The density can be derived from either on reservoir scale, either by analyzing the topology of the outcrop using scanlines (fig 5) or from the well (fig 12). Agbaje et al. (2023) showed that the coupled fracture density and k_{eff} display distinct behaviours related to the degree of connectivity and the degree of saturation of the networks. If the P_{21} is below a certain threshold value, the fractures are not connected and will not contribute to k_{eff}. This implies that the background network has no significant impact on fluid flow , and can thus be discarded on the scale of the reservoir. On the other hand, if the P_{21} is above a certain value, all fractures of the background network are practically connected, and adding more fractures to the network does not affect k_{eff}. This is the percolation threshold. As a consequence, the background network can be up-scaled as a matrix property on the reservoir scale , with a permeability of k_{eff}. It should be noted that the two threshold values in the curve depend on the statistics of the lengths of the fractures in the network (maximum and minimum length, and length distribution). The critical fracture density is between these two extremes, where small changes in density have a large effect on k_{eff}. In these cases, it is not possible to up-scale the background network directly, and explicit representation of the discontinuities is needed. This can be done with DFN-solvers based on statistical parameters (Kamel Targhi et al., 2024).

At the same time, the analysis of the BHI has shown that not all discontinuities network (e.g. Sanderson and Nixon, 2015; Hardebol et al., , or by numerically simulating flow through stochastically generated DFNs (e.g. Agbaje et al., 2023; Kamel Targhi et al., 2025) , the decision can be made to either represent the background explicitly or implicitly in reservoir scale models. After the significance of the background network is defined, the next step is to include the discontinuities observed in the well can that could not be placed in the framework of the background network. These discontinuities are thus likely created by local drivers and scale differently on the reservoir scale than the background network. As the background-related discontinuities are isolated from the dataset, the earlier discussed For example, if there are seismic-scale faults present in the subsurface, the above mentioned method of Maerten et al. (2016) is a suitable approach to model the remaining part of the discontinuities extrapolate these discontinuities to the reservoir scale.

This dynamic workflow will de-risk future geothermal drilling projects in different ways. The separate modeling of the permeability of the background network can be used to assess whether the background only can already produce economically viable fluid volumes, or if seismic-scale discontinuities are essential for production. Also, the well-placing strategy can be adjusted to the heterogeneity of the background permeability field. For example, in the Geneva Basin, most of the background discontinuities are striking NE-SW, and thus, a higher permeability in that direction is expected. A deviation of the well perpendicular to this strike will therefore likely optimize the well screen and thus the fluid inflow.

7 Conclusions

In this study, we presented a novel approach to connect outcrop studies of discontinuities with subsurface characterization of discontinuity networks. Associations of genetically related discontinuities that form the background network produced by the far-field stress are defined in the field. The regional character of the background network provides a robust link between analogue outcrops and subsurface target reservoirs. This link is used to improve interpretations of borehole images. By applying this methodology to analogue outcrops of a naturally fractured geothermal reservoir in the Geneva Basin, we have shown that:

1. ~~DAs are robust~~ Discontinuity associations are useful paleostress indicators that enable the reconstruction of the paleo stress field in which the background discontinuity network is formed
2. The regional character of the background network makes it a robust link between the outcrop and the subsurface
3. Analogue outcrops of the Lower Cretaceous carbonates in the Geneva Basin reveal two regional discontinuity-forming events that occurred before Alpine fold-and-thrusting
4. 40-50% of discontinuities observed on BHI from the target reservoir can be explained by the regional events that formed the background network, constrained by the work done on analogue outcrops
5. Outcrop ~~study is a time and cost-efficient method to obtain a~~ studies may provide a first-order evaluation of the contribution to flow of the background network in the subsurface.

Data availability. The measurements displayed in the stereonets of figure 8 are provided as a supplementary dataset.

Author contributions. JH: Writing - original draft preparation, Conceptualization, Methodology, Investigation, Data Curation, Visualization; POB: Conceptualization, Supervision, Writing - review and editing; GB: Conceptualization, Supervision, Writing - review and editing; MD: Formal Analysis; AM: Supervision, Writing - review and editing

Competing interests. The authors declare that they have no conflict of interest.

Acknowledgements. We would like to thank the Service Industriel de Geneve for making the BHI-data of the two wells in the Geneva Basin available to us. The first author is grateful for the Molengraaf Fonds for providing financial support for the conducted fieldwork. The assistance of Nil Feliu during the collection of the circular scanline data is highly appreciated. Didier Rigal and Jean-Marc Verdet are kindly thanked for sharing their endless knowledge on the Parmelan cave system, and for their guidance during the excursion in the Grotte de la Diau.

References

Agbaje, T. Q., Ghanbarian, B., and Hyman, J. D.: Effective Permeability in Fractured Reservoirs: Discrete Fracture Matrix Simulations and Percolation-Based Effective-Medium Approximation, Water Resources Research, 59, e2023WR036 505, https://doi.org/10.1029/2023WR036505, 2023.

Agosta, F., Alessandroni, M., Antonellini, M., Tondi, E., and Giorgioni, M.: From fractures to flow: A field-based quantitative analysis of an outcropping carbonate reservoir, Tectonophysics, 490, 197–213, https://doi.org/10.1016/j.tecto.2010.05.005, 2010.

Anderson, E.: The Dynamics of Faulting, Transactions of the Edinburgh Geological Society, 8, 387–402, https://doi.org/10.1144/transed.8.3.387, 1905.

Andrews, B. J., Roberts, J. J., Shipton, Z. K., Bigi, S., Tartarello, M. C., and Johnson, G.: How do we see fractures? Quantifying subjective bias in fracture data collection, Solid Earth, 10, 487–516, https://doi.org/10.5194/se-10-487-2019, 2019.

Angelier, J.: Inversion of Field Data in Fault Tectonics to Obtain the Regional Stress-III. A New Rapid Direct Inversion Method by Analytical Means, Geophysical Journal International, 103, 363–376, https://doi.org/10.1111/j.1365-246X.1990.tb01777.x, 1990.

Antunes, V., Planès, T., Zahradník, J., Obermann, A., Alvizuri, C., Carrier, A., and Lupi, M.: Seismotectonics and 1-D velocity model of the Greater Geneva Basin, France–Switzerland, Geophysical Journal International, 221, 2026–2047, https://doi.org/10.1093/gji/ggaa129, 2020.

Atkinson, G. M., Eaton, D. W., and Igonin, N.: Developments in understanding seismicity triggered by hydraulic fracturing, Nature Reviews Earth & Environment, 1, 264–277, https://doi.org/10.1038/s43017-020-0049-7, 2020.

Aubert, I., Lamarche, J., and Leonide, P.: Deciphering background fractures from damage fractures in fault zones and their effect on reservoir properties in microporous carbonates (Urgonian limestones, SE France), Petroleum Geoscience, 25, 443–453, https://doi.org/10.1144/petgeo2019-010, 2019.

Bai, T. and Pollard, D. D.: Fracture spacing in layered rocks: a new explanation based on the stress transition, Journal of Structural Geology, 22, 43–57, https://doi.org/10.1016/S0191-8141(99)00137-6, 2000.

Bauer, J. F., Krumbholz, M., Meier, S., and Tanner, D. C.: Predictability of properties of a fractured geothermal reservoir: the opportunities and limitations of an outcrop analogue study, Geothermal Energy, 5, 24, https://doi.org/10.1186/s40517-017-0081-0, 2017.

Beach, A.: The Geometry of En-Echelon Vein Arrays, Tectonophysics, 28, 245–263, https://doi.org/10.1016/0040-1951(75)90040-2, 1975.

Beaudoin, N., Lacombe, O., Bellahsen, N., and Emmanuel, L.: Contribution of Studies of Sub-Seismic Fracture Populations to Paleo-Hydrological Reconstructions (Bighorn Basin, USA), Procedia Earth and Planetary Science, 7, 57–60, https://doi.org/10.1016/j.proeps.2013.03.198, 2013.

Beaudoin, N., Koehn, D., Lacombe, O., Lecouty, A., Billi, A., Aharonov, E., and Parlangeau, C.: Fingerprinting stress: Stylolite and calcite twinning paleopiezometry revealing the complexity of progressive stress patterns during folding—The case of the Monte Nero anticline in the Apennines, Italy, Tectonics, 35, 1687–1712, https://doi.org/10.1002/2016TC004128, 2016.

Bellahsen, N., Mouthereau, F., Boutoux, A., Bellanger, M., Lacombe, O., Jolivet, L., and Rolland, Y.: Collision Kinematics in the Western External Alps: Kinematics of the Alpine Collision, Tectonics, 33, 1055–1088, https://doi.org/10.1002/2013TC003453, 2014.

Bergbauer, S. and Pollard, D. D.: A new conceptual fold-fracture model including prefolding joints, based on the Emigrant Gap anticline, Wyoming, Geological Society of America Bulletin, 116, 294, https://doi.org/10.1130/B25225.1, 2004.

Berio, L. R., Storti, F., Balsamo, F., Mittempergher, S., Bistacchi, A., and Meda, M.: Structural Evolution of the Parmelan Anticline (Bornes Massif, France): Recording the Role of Structural Inheritance and Stress Field Changes on the Finite Deformation Pattern, Tectonics, 40, e2021TC006 913, https://doi.org/10.1029/2021TC006913, 2021.

Berio, L. R., Mittempergher, S., Storti, F., Bernasconi, S. M., Cipriani, A., Lugli, F., and Balsamo, F.: Open–Closed–Open Palaeofluid System Conditions Recorded in the Tectonic Vein Networks of the Parmelan Anticline (Bornes Massif, France), Journal of the Geological Society, 179, jgs2021–117, https://doi.org/10.1144/jgs2021-117, 2022.

Berre, I., Doster, F., and Keilegavlen, E.: Flow in Fractured Porous Media: A Review of Conceptual Models and Discretization Approaches, Transport in Porous Media, 130, 215–236, https://doi.org/10.1007/s11242-018-1171-6, 2019.

Bertotti, G., De Graaf, S., Bisdom, K., Oskam, B., B. Vonhof, H., H. R. Bezerra, F., J. G. Reijmer, J., and L. Cazarin, C.: Fracturing and Fluid-flow during Post-rift Subsidence in Carbonates of the Jandaíra Formation, Potiguar Basin, NE Brazil, Basin Research, 29, 836–853, https://doi.org/10.1111/bre.12246, 2017.

Bisdom, K., Bertotti, G., and Nick, H. M.: A Geometrically Based Method for Predicting Stress-Induced Fracture Aperture and Flow in Discrete Fracture Networks, AAPG Bulletin, 100, 1075–1097, https://doi.org/10.1306/02111615127, 2016.

Bond, C., Gibbs, A., Shipton, Z., and Jones, S.: What do you think this is? "Conceptual uncertainty" in geoscience interpretation, GSA Today, 17, 4, https://doi.org/10.1130/GSAT01711A.1, 2007.

Brentini, M.: Impact d'une donnée géologique hétérogène dans la gestion des géo-ressources: analyse intégrée et valorisation de la stratigraphie à travers le bassin genevois (Suisse, France), Ph.D. thesis, Université de Genève, https://doi.org/10.13097/ARCHIVE-OUVERTE/UNIGE:103409, 2018.

Bruna, P.-O., Lavenu, A. P., Matonti, C., and Bertotti, G.: Are stylolites fluid-flow efficient features?, Journal of Structural Geology, 125, 270–277, https://doi.org/10.1016/j.jsg.2018.05.018, 2019.

Butler, R. W. H.: Hydrocarbon Maturation, Migration and Tectonic Loading in the Western Alpine Foreland Thrust Belt, Geological Society, London, Special Publications, 59, 227–244, https://doi.org/10.1144/GSL.SP.1991.059.01.15, 1991.

Caine, J. S., Evans, J. P., and Forster, C. B.: Fault zone architecture and permeability structure, Geology, 24, 1025, https://doi.org/10.1130/0091-7613(1996)024<1025:FZAAPS>2.3.CO;2, 1996.

Cao, M. and Sharma, M. M.: The impact of changes in natural fracture fluid pressure on the creation of fracture networks, Journal of Petroleum Science and Engineering, 216, 110 783, https://doi.org/10.1016/j.petrol.2022.110783, 2022.

Casini, G., Gillespie, P., Vergés, J., Romaire, I., Fernández, N., Casciello, E., Saura, E., Mehl, C., Homke, S., Embry, J.-C., Aghajari, L., and Hunt, D. W.: Sub-seismic fractures in foreland fold and thrust belts: insight from the Lurestan Province, Zagros Mountains, Iran, Petroleum Geoscience, 17, 263–282, https://doi.org/10.1144/1354-079310-043, 2011.

Cederbom, C. E., Sinclair, H. D., Schlunegger, F., and Rahn, M. K.: Climate-Induced Rebound and Exhumation of the European Alps, Geology, 32, 709, https://doi.org/10.1130/G20491.1, 2004.

Charollais, J., Mastrangelo, B., Strasser, A., Piuz, A., Granier, B., Monteil, E., Ruchat, C., and Savoy, L.: Lithostratigraphie, biostratigraphie, cartographie et géologie structurale du Mont Salève, entre l'Arve et les Usses (Haute Savoie, France), Revue de Paleobiologie, 42, 1–127, https://doi.org/10.5281/ZENODO.7446048, 2023.

Chatterjee, S. and Mukherjee, S.: Review on drilling-induced fractures in drill cores, Marine and Petroleum Geology, 151, 106 089, https://doi.org/10.1016/j.marpetgeo.2022.106089, 2023.

Chemenda, A. I.: Bed thickness-dependent fracturing and inter-bed coupling define the nonlinear fracture spacing-bed thickness relationship in layered rocks: Numerical modeling, Journal of Structural Geology, 165, 104 741, https://doi.org/10.1016/j.jsg.2022.104741, 2022.

Clavel, B., Charollais, J., Conrad, M., Du Chêne, R. J., Busnardo, R., Gardin, S., Erba, E., Schroeder, R., Cherchi, A., Decrouez, D., Granier, B., Sauvagnat, J., and Weidmann, M.: Dating and Progradation of the Urgonian Limestone from the Swiss Jura to South-East France, Zeitschrift der Deutschen Gesellschaft für Geowissenschaften, 158, 1025–1062, https://doi.org/10.1127/1860-1804/2007/0158-1025, 2007.

Clavel, B., Conrad, M. A., Busnardo, R., Charollais, J., and Granier, B.: Mapping the Rise and Demise of Urgonian Platforms (Late Hauterivian - Early Aptian) in Southeastern France and the Swiss Jura, Cretaceous Research, 39, 29–46, https://doi.org/10.1016/j.cretres.2012.02.009, 2013.

Clerc, N. and Moscariello, A.: A Revised Structural Framework for the Geneva Basin and the Neighboring France Region as Revealed from 2D Seismic Data: Implications for Geothermal Exploration, Swiss Bulletin für angewandte Geologie, 2020.

Crampton, S. and Allen, P.: Recognition of Forebulge Unconformities Associated with Early Stage Foreland Basin Development: Example from the North Alpine Foreland Basin, AAPG Bulletin, 79, 1495–1514, https://doi.org/10.1306/7834DA1C-1721-11D7-8645000102C1865D, 1995.

Deville, E. and Sassi, W.: Contrasting Thermal Evolution of Thrust Systems: An Analytical and Modeling Approach in the Front of the Western Alps, AAPG Bulletin, 90, 887–907, https://doi.org/10.1306/01090605046, 2006.

Doesburg, M.: Uncertainty Reduction in Image Log Fracture Interpretation, and Its Implications to the Geological History of the Geneva Basin, Switzerland, Master's thesis, TU Delft, Delft, https://resolver.tudelft.nl/uuid:a16d4d2b-d373-48a7-9e5c-b6f22d3045d0, 2023.

Elliott, S. J., Forstner, S. R., Wang, Q., Corrêa, R., Shakiba, M., Fulcher, S. A., Hebel, N. J., Lee, B. T., Tirmizi, S. T., Hooker, J. N., Fall, A., Olson, J. E., and Laubach, S. E.: Diagenesis is key to unlocking outcrop fracture data suitable for quantitative extrapolation to geothermal targets, Frontiers in Earth Science, 13, 1545 052, https://doi.org/10.3389/feart.2025.1545052, 2025.

Engelder, T.: Loading paths to joint propagation during a tectonic cycle: an example from the Appalachian Plateau, U.S.A., Journal of Structural Geology, 7, 459–476, https://doi.org/10.1016/0191-8141(85)90049-5, 1985.

English, J. M.: Thermomechanical origin of regional fracture systems, AAPG Bulletin, 96, 1597–1625, https://doi.org/10.1306/01021211018, 2012.

Eruteya, O. E., Crinière, A., and Moscariello, A.: Seismic expression of paleokarst morphologies and associated Siderolithic infill in the Geneva Basin, Switzerland: Implications for geothermal exploration, Geothermics, 117, 102 868, https://doi.org/10.1016/j.geothermics.2023.102868, 2024.

Fadel, M., Meneses Rioseco, E., Bruna, P.-O., and Moeck, I.: Pressure transient analysis to investigate a coupled fracture corridor and a fault damage zone causing an early thermal breakthrough in the North Alpine Foreland Basin, Geoenergy Science and Engineering, 229, 212 072, https://doi.org/10.1016/j.geoen.2023.212072, 2023.

Fernández-Ibáñez, F., DeGraff, J., and Ibrayev, F.: Integrating borehole image logs with core: A method to enhance subsurface fracture characterization, AAPG Bulletin, 102, 1067–1090, https://doi.org/10.1306/0726171609317002, 2018.

Genter, A., Castaing, C., Dezayes, C., Tenzer, H., Traineau, H., and Villemin, T.: Comparative analysis of direct (core) and indirect (borehole imaging tools) collection of fracture data in the Hot Dry Rock Soultz reservoir (France), Journal of Geophysical Research: Solid Earth, 102, 15 419–15 431, https://doi.org/10.1029/97JB00626, 1997.

Grare, A., Lacombe, O., Mercadier, J., Benedicto, A., Guilcher, M., Trave, A., Ledru, P., and Robbins, J.: Fault Zone Evolution and Development of a Structural and Hydrological Barrier: The Quartz Breccia in the Kiggavik Area (Nunavut, Canada) and Its Control on Uranium Mineralization, Minerals, 8, 319, https://doi.org/10.3390/min8080319, 2018.

Groshong, R. H.: Strain, fractures, and pressure solution in natural single-layer folds, Geological Society of America Bulletin, 86, 1363, https://doi.org/10.1130/0016-7606(1975)86<1363:SFAPSI>2.0.CO;2, 1975.

Guglielmetti, L. and Moscariello, A.: On the Use of Gravity Data in Delineating Geologic Features of Interest for Geothermal Exploration in the Geneva Basin (Switzerland): Prospects and Limitations, Swiss Journal of Geosciences, 114, 15, https://doi.org/10.1186/s00015-021-00392-8, 2021.

Guglielmetti, L., Poletto, F., Corubolo, P., Bitri, A., Dezayes, C., Farina, B., Martin, F., Meneghini, F., Moscariello, A., Nawratil De Bono, C., and Schleifer, A.: Results of a Walk-above Vertical Seismic Profiling Survey Acquired at the Thônex-01 Geothermal Well (Switzerland) to Delineate Fractured Carbonate Formations for Geothermal Development, Geophysical Prospecting, 68, 1139–1153, https://doi.org/10.1111/1365-2478.12912, 2020.

Guglielmetti, L., Houlié, N., de Bono, C. N., Martin, F., Coudroit, J., Oerlemans, P., and Cremer, H.: HEATSTORE D5.2: Monitoring Results for the Geneva HT-ATES Case-Study, HEATSTORE project report, 2021.

Hancock, P.: Brittle Microtectonics: Principles and Practice, Journal of Structural Geology, 7, 437–457, https://doi.org/10.1016/0191-8141(85)90048-3, 1985.

Hardebol, N. J., Maier, C., Nick, H., Geiger, S., Bertotti, G., and Boro, H.: Multiscale fracture network characterization and impact on flow: A case study on the Latemar carbonate platform, Journal of Geophysical Research: Solid Earth, 120, 8197–8222, https://doi.org/10.1002/2015JB011879, 2015.

Heap, M. J., Baud, P., Reuschlé, T., and Meredith, P. G.: Stylolites in limestones: Barriers to fluid flow?, Geology, 42, 51–54, https://doi.org/10.1130/G34900.1, 2014.

Homberg, C., Lacombe, O., Angelier, J., and Bergerat, F.: New Constraints for Indentation Mechanisms in Arcuate Belts from the Jura Mountains, France, Geology, 27, 827, https://doi.org/10.1130/0091-7613(1999)027<0827:NCFIMI>2.3.CO;2, 1999.

Homberg, C., Bergerat, F., Philippe, Y., Lacombe, O., and Angelier, J.: Structural Inheritance and Cenozoic Stress Fields in the Jura Fold-and-Thrust Belt (France), Tectonophysics, 357, 137–158, https://doi.org/10.1016/S0040-1951(02)00366-9, 2002.

Hooker, J. N., Gomez, L. A., Laubach, S. E., Gale, J. F. W., and Marrett, R.: Effects of diagenesis (cement precipitation) during fracture opening on fracture aperture-size scaling in carbonate rocks, Geological Society, London, Special Publications, 370, 187–206, https://doi.org/10.1144/SP370.9, 2012.

Hosseinzadeh, S., Kadkhodaie, A., Wood, D. A., Rezaee, R., and Kadkhodaie, R.: Discrete fracture modeling by integrating image logs, seismic attributes, and production data: a case study from Ilam and Sarvak Formations, Danan Oilfield, southwest of Iran, Journal of Petroleum Exploration and Production Technology, 13, 1053–1083, https://doi.org/10.1007/s13202-022-01586-y, 2023.

Jenny, J., Burri, J., Mural, R., Pugin, A., Schegg, R., and Ugemach, P.: Le Forage Geothermique de Thonex-01 (Canton de Geneve): Aspects Stratigraphiques, Tectoniques, Diagenetiques, Geophysiques et Hydrogeologiques, Eclogae Geologicae Helvetiae, 88, 265–396, 1995.

Kalifi, A., Leloup, P. H., Sorrel, P., Galy, A., Demory, F., Spina, V., Huet, B., Quillévéré, F., Ricciardi, F., Michoux, D., Lecacheur, K., Grime, R., Pittet, B., and Rubino, J.-L.: Chronology of Thrust Propagation from an Updated Tectono-Sedimentary Framework of the Miocene Molasse (Western Alps), Solid Earth, 12, 2735–2771, https://doi.org/10.5194/se-12-2735-2021, 2021.

Kamel Targhi, E., Bruna, P.-O., Daniilidis, A., Rongier, G., and Geiger, S.: GeoDFN - A Flexible, Open-Source Software for Generating Geologically Consistent Discrete Fracture Networks, https://doi.org/10.4121/0DC9C47A-2294-4811-A0FE-E049CB15FF3D.V1, 2024.

Kamel Targhi, E., Bruna, P.-O., Daniilidis, A., Rongier, G., and Geiger, S.: From outcrop observations to dynamic simulations: an efficient workflow for generating ensembles of geologically plausible fracture networks and assessing their impact on flow and transport, Geoenergy, 3, geoenergy2025–028, https://doi.org/10.1144/geoenergy2025-028, 2025.

Koehn, D., Rood, M., Beaudoin, N., Chung, P., Bons, P., and Gomez-Rivas, E.: A new stylolite classification scheme to estimate compaction and local permeability variations, Sedimentary Geology, 346, 60–71, https://doi.org/10.1016/j.sedgeo.2016.10.007, 2016.

La Bruna, V., Lamarche, J., Agosta, F., Rustichelli, A., Giuffrida, A., Salardon, R., and Marié, L.: Structural diagenesis of shallow platform carbonates: Role of early embrittlement on fracture setting and distribution, case study of Monte Alpi (Southern Apennines, Italy), Journal of Structural Geology, 131, 103 940, https://doi.org/10.1016/j.jsg.2019.103940, 2020.

La Bruna, V., Bezerra, F. H., Souza, V. H., Maia, R. P., Auler, A. S., Araujo, R. E., Cazarin, C. L., Rodrigues, M. A., Vieira, L. C., and Sousa, M. O.: High-permeability zones in folded and faulted silicified carbonate rocks – Implications for karstified carbonate reservoirs, Marine and Petroleum Geology, 128, 105 046, https://doi.org/10.1016/j.marpetgeo.2021.105046, 2021.

Lacombe, O., Bellahsen, N., and Mouthereau, F.: Fracture patterns in the Zagros Simply Folded Belt (Fars, Iran): constraints on early collisional tectonic history and role of basement faults, Geological Magazine, 148, 940–963, https://doi.org/10.1017/S001675681100029X, 2011.

Lacombe, O., Beaudoin, N. E., Hoareau, G., Labeur, A., Pecheyran, C., and Callot, J.-P.: Dating folding beyond folding, from layer-parallel shortening to fold tightening, using mesostructures: lessons from the Apennines, Pyrenees, and Rocky Mountains, Solid Earth, 12, 2145–2157, https://doi.org/10.5194/se-12-2145-2021, 2021.

Lamarche, J., Lavenu, A. P., Gauthier, B. D., Guglielmi, Y., and Jayet, O.: Relationships between fracture patterns, geodynamics and mechanical stratigraphy in Carbonates (South-East Basin, France), Tectonophysics, 581, 231–245, https://doi.org/10.1016/j.tecto.2012.06.042, 2012.

Lander, R. H. and Laubach, S. E.: Insights into rates of fracture growth and sealing from a model for quartz cementation in fractured sandstones, Geological Society of America Bulletin, 127, 516–538, https://doi.org/10.1130/B31092.1, 2015.

Laubach, S. E., Baumgardner, R. W., Monson, E. R., Hunt, E., and Meador, K. J.: Fracture Detection in Low-Permeability Reservoir Sandstone: A Comparison of BHTV and FMS Logs to Core, in: SPE Annual Technical Conference and Exhibition, pp. SPE–18 119–MS, SPE, Houston, Texas, https://doi.org/10.2118/18119-MS, 1988.

Laubach, S. E., Olson, J. E., and Gross, M. R.: Mechanical and fracture stratigraphy, AAPG Bulletin, 93, 1413–1426, https://doi.org/10.1306/07270909094, 2009.

Laubach, S. E., Lander, R. H., Criscenti, L. J., Anovitz, L. M., Urai, J. L., Pollyea, R. M., Hooker, J. N., Narr, W., Evans, M. A., Kerisit, S. N., Olson, J. E., Dewers, T., Fisher, D., Bodnar, R., Evans, B., Dove, P., Bonnell, L. M., Marder, M. P., and Pyrak-Nolte, L.: The Role of Chemistry in Fracture Pattern Development and Opportunities to Advance Interpretations of Geological Materials, Reviews of Geophysics, 57, 1065–1111, https://doi.org/10.1029/2019RG000671, 2019.

Lavenu, A. P. and Lamarche, J.: What controls diffuse fractures in platform carbonates? Insights from Provence (France) and Apulia (Italy), Journal of Structural Geology, 108, 94–107, https://doi.org/10.1016/j.jsg.2017.05.011, 2018.

Lee, S. H., Lough, M. F., and Jensen, C. L.: Hierarchical modeling of flow in naturally fractured formations with multiple length scales, Water Resources Research, 37, 443–455, https://doi.org/10.1029/2000WR900340, 2001.

Lismonde, B.: Le réseau de la Diau, Karstologia : revue de karstologie et de spéléologie physique, 1, 9–18, https://doi.org/10.3406/karst.1983.2034, 1983.

Looser, N., Madritsch, H., Guillong, M., Laurent, O., Wohlwend, S., and Bernasconi, S. M.: Absolute Age and Temperature Constraints on Deformation Along the Basal Décollement of the Jura Fold-and-Thrust Belt From Carbonate U-Pb Dating and Clumped Isotopes, Tectonics, 40, e2020TC006 439, https://doi.org/10.1029/2020TC006439, 2021.

Lorenz, J. C. and Cooper, S. P.: Atlas of Natural and Induced Fractures in Core, Wiley, 1 edn., ISBN 978-1-119-16000-7 978-1-119-16001-4, https://doi.org/10.1002/9781119160014, 2017.

Maerten, L., Gillespie, P., and Daniel, J.-M.: Three-Dimensional Geomechanical Modeling for Constraint of Subseismic Fault Simulation, AAPG Bulletin, 90, 1337–1358, https://doi.org/10.1306/03130605148, 2006.

Maerten, L., Maerten, F., Lejri, M., and Gillespie, P.: Geomechanical Paleostress Inversion Using Fracture Data, Journal of Structural Geology, 89, 197–213, https://doi.org/10.1016/j.jsg.2016.06.007, 2016.

Marro, A., Hauvette, L., Borderie, S., and Mosar, J.: Tectonics of the Western Internal Jura Fold-and-Thrust Belt: 2D Kinematic Forward Modelling, Swiss Journal of Geosciences, 116, 10, https://doi.org/10.1186/s00015-023-00435-2, 2023.

Masson, M.: Le karst du Parmelan, Haute-Savoie, relations fracturation-karstification, Karstologia : revue de karstologie et de spéléologie physique, 5, 3–8, https://doi.org/10.3406/karst.1985.2081, 1985.

Mauldon, M., Dunne, W., and Rohrbaugh, M.: Circular Scanlines and Circular Windows: New Tools for Characterizing the Geometry of Fracture Traces, Journal of Structural Geology, 23, 247–258, https://doi.org/10.1016/S0191-8141(00)00094-8, 2001.

Medici, G., Ling, F., and Shang, J.: Review of Discrete Fracture Network Characterization for Geothermal Energy Extraction, Frontiers in Earth Science, 11, 1328 397, https://doi.org/10.3389/feart.2023.1328397, 2023.

Moscariello, A.: Exploring for Geo-Energy Resources in the Geneva Basin (Western Switzerland): Opportunities and Challenges, Swiss Bulletin für angewandte Geologie, 24, 105–124, http://archive-ouverte.unige.ch/unige:131617, 2019.

Moss, S.: Organic Maturation in the French Subalpine Chains: Regional Differences in Burial History and the Size of Tectonic Loads, Journal of the Geological Society, 149, 503–515, https://doi.org/10.1144/gsjgs.149.4.0503, 1992.

Pascal, C.: Paleostress inversion techniques: Methods and applications for tectonics, Elsevier, 2021.

Peacock, D., Sanderson, D., and Rotevatn, A.: Relationships between fractures, Journal of Structural Geology, 106, 41–53, https://doi.org/10.1016/j.jsg.2017.11.010, 2018.

Peacock, D. C., Sanderson, D. J., Bastesen, E., Rotevatn, A., and Storstein, T. H.: Causes of Bias and Uncertainty in Fracture Network Analysis, Norwegian Journal of Geology, https://doi.org/10.17850/njg99-1-06, 2019.

Peacock, D. C. P., Sanderson, D. J., and Leiss, B.: Use of Analogue Exposures of Fractured Rock for Enhanced Geothermal Systems, Geosciences, 12, 318, https://doi.org/10.3390/geosciences12090318, 2022.

Petit, J.-P., Chemenda, A. I., Minisini, D., Richard, P., Bergman, S. C., and Gross, M.: When Do Fractures Initiate during the Geological History of a Sedimentary Basin? Test Case of a Loading-Fracturing Path Methodology, Journal of Structural Geology, 164, 104 683, https://doi.org/10.1016/j.jsg.2022.104683, 2022.

Price, N.: Fault and joint development in brittle and semi-brittle rock. [., Pergamon, Oxford, 1966.

Procter, A. and Sanderson, D. J.: Spatial and layer-controlled variability in fracture networks, Journal of Structural Geology, 108, 52–65, https://doi.org/10.1016/j.jsg.2017.07.008, 2018.

Rusillon, E.: Characterisation and rock typing of deep geothermal reservoirs in the Greater Geneva Basin (Switzerland & France), Ph.D. thesis, Université de Genève, https://doi.org/10.13097/ARCHIVE-OUVERTE/UNIGE:105286, 2017.

Rysak, B., Gale, J. F. W., Laubach, S. E., and Ferrill, D. A.: Mechanisms for the Generation of Complex Fracture Networks: Observations From Slant Core, Analog Models, and Outcrop, Frontiers in Earth Science, 10, 848 012, https://doi.org/10.3389/feart.2022.848012, 2022.

Sanderson, D. J.: Field-based structural studies as analogues to sub-surface reservoirs, Geological Society, London, Special Publications, 436, 207–217, https://doi.org/10.1144/SP436.5, 2016.

Sanderson, D. J. and Nixon, C. W.: The use of topology in fracture network characterization, Journal of Structural Geology, 72, 55–66, https://doi.org/10.1016/j.jsg.2015.01.005, 2015.

Sanderson, D. J., Peacock, D. C., and Nixon, C. W.: Fracture sets and sequencing, Earth-Science Reviews, 257, 104 888, https://doi.org/10.1016/j.earscirev.2024.104888, 2024.

Schegg, R. and Leu, W.: Analysis of Erosion Events and Palaeogeothermal Gradients in the North Alpine Foreland Basin of Switzerland, Geological Society, London, Special Publications, 141, 137–155, https://doi.org/10.1144/GSL.SP.1998.141.01.09, 1998.

Simpson, R. W.: Quantifying Anderson's Fault Types, Journal of Geophysical Research: Solid Earth, 102, 17 909–17 919, https://doi.org/10.1029/97JB01274, 1997.

Smeraglia, L., Looser, N., Fabbri, O., Choulet, F., Guillong, M., and Bernasconi, S. M.: U–Pb Dating of Middle Eocene–Pliocene Multiple Tectonic Pulses in the Alpine Foreland, Solid Earth, 12, 2539–2551, https://doi.org/10.5194/se-12-2539-2021, 2021.

Smeraglia, L., Fabbri, O., Choulet, F., Jaggi, M., and Bernasconi, S. M.: The Role of Thrust and Strike-Slip Faults in Controlling Regional-Scale Paleofluid Circulation in Fold-and-Thrust Belts: Insights from the Jura Mountains (Eastern France), Tectonophysics, 829, 229 299, https://doi.org/10.1016/j.tecto.2022.229299, 2022.

Solano, N., Zambrano, L., and Aguilera, R.: Cumulative-Gas-Production Distribution on the Nikanassin Tight Gas Formation, Alberta and British Columbia, Canada, SPE Reservoir Evaluation & Engineering, 14, 357–376, https://doi.org/10.2118/132923-PA, 2011.

Sommaruga, A., Mosar, J., Schori, M., and Gruber, M.: The Role of the Triassic Evaporites Underneath the North Alpine Foreland, in: Permo-Triassic Salt Provinces of Europe, North Africa and the Atlantic Margins, pp. 447–466, Elsevier, ISBN 978-0-12-809417-4, https://doi.org/10.1016/B978-0-12-809417-4.00021-5, 2017.

Strasser, A., Charollais, J., Conrad, M. A., Clavel, B., Pictet, A., and Mastrangelo, B.: The Cretaceous of the Swiss Jura Mountains: An Improved Lithostratigraphic Scheme, Swiss Journal of Geosciences, 109, 201–220, https://doi.org/10.1007/s00015-016-0215-6, 2016.

Torabi, A. and Berg, S. S.: Scaling of fault attributes: A review, Marine and Petroleum Geology, 28, 1444–1460, https://doi.org/10.1016/j.marpetgeo.2011.04.003, 2011.

Toussaint, R., Aharonov, E., Koehn, D., Gratier, J.-P., Ebner, M., Baud, P., Rolland, A., and Renard, F.: Stylolites: A review, Journal of Structural Geology, 114, 163–195, https://doi.org/10.1016/j.jsg.2018.05.003, 2018.

Tutuarima, F., Cecchetti, E., Abels, H., Bertotti, G., and Bruna, P.: Main controls on natural fracture distribution in the Lower Triassic sandstones of the West Netherlands Basin, in: 84th EAGE Annual Conference & Exhibition, pp. 1–5, European Association of Geoscientists & Engineers, Vienna, Austria,, https://doi.org/10.3997/2214-4609.2023101051, 2023.

Ukar, E., Laubach, S. E., and Hooker, J. N.: Outcrops as Guides to Subsurface Natural Fractures: Example from the Nikanassin Formation Tight-Gas Sandstone, Grande Cache, Alberta Foothills, Canada, Marine and Petroleum Geology, 103, 255–275, https://doi.org/10.1016/j.marpetgeo.2019.01.039, 2019.

Watkins, H., Bond, C. E., Healy, D., and Butler, R. W. H.: Appraisal of Fracture Sampling Methods and a New Workflow to Characterise Heterogeneous Fracture Networks at Outcrop, Journal of Structural Geology, 72, 67–82, https://doi.org/10.1016/j.jsg.2015.02.001, 2015a.

Watkins, H., Butler, R. W., Bond, C. E., and Healy, D.: Influence of structural position on fracture networks in the Torridon Group, Achnashellach fold and thrust belt, NW Scotland, Journal of Structural Geology, 74, 64–80, https://doi.org/10.1016/j.jsg.2015.03.001, 2015b.

Williams, J. H. and Johnson, C. D.: Acoustic and optical borehole-wall imaging for fractured-rock aquifer studies, Journal of Applied Geophysics, 55, 151–159, https://doi.org/10.1016/j.jappgeo.2003.06.009, 2004.

Zang, A., Oye, V., Jousset, P., Deichmann, N., Gritto, R., McGarr, A., Majer, E., and Bruhn, D.: Analysis of induced seismicity in geothermal reservoirs – An overview, Geothermics, 52, 6–21, https://doi.org/10.1016/j.geothermics.2014.06.005, 2014.

Zarian, P. and Dymmock, S.: Conceptual Uncertainty in Geological Interpretation of Borehole Image Logs, in: 72nd EAGE Conference and Exhibition incorporating SPE EUROPEC 2010, European Association of Geoscientists & Engineers, Barcelona, Spain,, ISBN 978-90-73781-86-3, https://doi.org/10.3997/2214-4609.201400973, 2010.